



Comparison of fresh and browning lotus roots (*Nelumbo nucifera* Gaertn.) on modulating cholesterol metabolism via decreasing hepatic cholesterol deposition and increasing fecal bile acid excretion

Jingfang Li^{a,c}, Ting Luo^a, Xiaoping Li^a, Xiaoru Liu^{a,*}, Ze-yuan Deng^{a,b,**}

^a State Key Laboratory of Food Science and Resources, Nanchang University, Nanchang, Jiangxi, 330047, China

^b Institute for Advanced Study, Nanchang University, Nanchang, Jiangxi, 330031, China

^c Department of Food Science and Technology, Science Drive 2, Faculty of Science, National University of Singapore, 117542, Singapore

ARTICLE INFO

Handling Editor: Dr. Quancai Sun

Keywords:

Lotus root
Browning lotus root
FXR-FGF15
Cholesterol metabolism

ABSTRACT

Lotus root (LR) is prone to browning after harvest due to the oxidation of phenolic compounds by polyphenol oxidase (PPO). This study compared the effects of LR extract and BLR extract on cholesterol metabolism in high-fat diet (HFD) mice. Our findings highlighted the innovative potentiality of BLR extract in effectively regulating cholesterol metabolism via inhibiting the intestinal FXR-FGF15 signaling pathway and boosting probiotics in gut microbiota, offering valuable insights for hypercholesterolemia and metabolic disorders. In detail, catechin was the main phenolic compound in LR, while after browning, theaflavin was the main oxidation product of phenolic compounds in BLR. Both the intake of LR extract and BLR extract regulated the disorder of cholesterol metabolism induced by HFD. In particular, BLR extract intake exhibited more robust effects on increasing the BAs contents synthesized in the liver and excreted in feces compared with LR extract intake. Furthermore, the consumption of BLR extract was more effective than that of LR extract in reducing the ileal protein expressions of FXR and FGF15 and shifting BAs biosynthesis from the classical pathway to the alternative pathway. Moreover, LR extract and BLR extract had distinct effects on the gut microbiota in HFD-fed mice: BLR extract significantly elevated probiotics *Akkermansia* abundance, while LR extract increased *Lactobacillus* abundance. Therefore, both LR extract and BLR extract improved the cholesterol deposition effectively and BLR extract even showed a stronger effect on regulating key gene and protein expressions of cholesterol metabolism.

1. Introduction

Nowadays, the excessive consumption of high-fat and high-cholesterol foods has become a major public health issue. High-fat and high-cholesterol diets lead to an increase in both hepatic and plasma cholesterol levels, and even cause the development of obesity, hyperlipidemia, non-alcoholic fatty liver disease, and hepatocellular carcinoma (Clifford et al., 2021). However, the currently used drugs, such as statins, a class of drugs frequently prescribed to lower cholesterol, cause side effects including hepatotoxicity, renal toxicity, and other diseases (Ward et al., 2019). These drugs primarily target cholesterol synthesis in the liver (Stancu and Sima, 2001). In contrast, phenolic compounds, abundantly found in natural foods, offer a safer and more comprehensive approach to cholesterol management by inhibiting cholesterol

absorption in the intestines (Ikeda et al., 2010; Zanotti et al., 2015). Additionally, phenolic compounds can complement traditional medications, potentially reducing drug dosages and associated side effects while enhancing overall cholesterol management efficacy (Mahfuz et al., 2021; Park et al., 2002; Toma et al., 2020).

Lotus root (*Nelumbo nucifera* Gaertn., LR), which is widely planted in Asia, is an aquatic vegetable with high nutritional and economic value. There are rich nutrients including starch, sugars, dietary fiber, flavonoids, and phenolic compounds in LR (Limwachiranon et al., 2018; Showkat et al., 2021). Studies suggested that the phytochemicals like flavonoids and phenolic compounds in LR have various health promoting benefits such as reducing the risk of obesity, exhibiting antioxidant activity (You et al., 2014), and preventing the development and progression of NAFLD (Tsuruta et al., 2012). In detail, catechin

* Corresponding author.

** Corresponding author. State Key Laboratory of Food Science and Resources, Nanchang University, Nanchang, Jiangxi, 330047, China.

E-mail addresses: liuxiaoru@ncu.edu.cn (X. Liu), dengzy@ncu.edu.cn (Z.-y. Deng).

<https://doi.org/10.1016/j.crf.2023.100630>

Received 17 July 2023; Received in revised form 23 September 2023; Accepted 30 October 2023

Available online 2 November 2023

2665-9271/© 2023 Published by Elsevier B.V. This is an open access article under the CC BY-NC-ND license (<http://creativecommons.org/licenses/by-nc-nd/4.0/>).

improved higher levels of fatness, blood pressure, and cholesterol in children (Tsuruta et al., 2012). Caffeic acid prevented hyperlipidemia and obesity in C57BL/6 mice by regulating the expression of liver adipogenic genes (Liao et al., 2013). Epicatechin can regulate blood lipids and attenuate hepatic steatosis (Cheng et al., 2017). However, LR is susceptible to browning by polyphenol oxidase (PPO) after storage or being cut, which may cause changes in the phytochemicals of LR, especially the oxidized phenolic compounds. The browning of LR is normally thought as the deterioration of quality, which results in a large amount of waste and economic loss of lotus resources. However, it is worth noting that previous studies also indicated the total phenolic content (TPC) of LR increased during browning storage at 20 °C (Min et al., 2017), while few studies elaborated the changes of the main oxidized phenolic products in browning LR (BLR). Actually, some of the oxidized phenolic products or phenolic derivatives are still regarded as natural substances with numerous advantageous biological effects. Theaflavin, as an oxidation product of catechins, offers a range of health benefits, including anti-obesity effects (Jin et al., 2013), the attenuation of hypercholesterolemia (Huang et al., 2019), the alleviation of hepatic lipid accumulation (Lin et al., 2007), and the prevention of diabetes onset (Li et al., 2021). Forsythoside A, a derivative of caffeic acid, enhanced antioxidant status, meat fatty acid deposition, and influenced the composition of the intestinal microbial community (Liu et al., 2022). Our previous study also reported the BLR extract can promote cholesterol metabolism in free fatty acids-induced HepG2 cells (Zhong et al., 2023). Based on these research findings, the bioactive compounds in BLR and their potential benefits deserve further investigation, which is a good way to recycle the waste of lotus resources.

Reducing cholesterol deposition in the liver is a typical way to regulate cholesterol metabolism and the conversion of cholesterol into bile acids (BAs) is a vital process for hepatocytes to remove hepatic cholesterol (Ling et al., 2019). In the liver, cholesterol is metabolized into BAs mainly via two main biosynthetic pathways, the classical pathway and the alternative pathway (Pandak and Kakiyama, 2019). Cholesterol 7 α -hydroxylase (CYP7A1) and cholesterol 12 α -hydroxylase (CYP8B1) are the key enzymes in the classical pathway of cholesterol catabolism, while sterol 27-hydroxylase (CYP27A1) and oxysterol 7 α -hydroxylase (CYP7B1) are typical enzymes in the alternative pathway. The BAs enterohepatic circulation is the flow of BAs in the liver, bile duct, and intestinal tract, as well as its reabsorption and reuse. The decrease in intestinal reabsorption of BA and the increase in excretion of BAs through feces promote the degradation of cholesterol in the liver through negative feedback regulation (Dawson, 2018). The Farnesoid X receptor (FXR), a nuclear receptor, is regarded as a key factor in the regulation of BAs synthesis and secretion (Guo et al., 2022). This intricate process initiates within the ileum, where BAs activate the FXR. The activation subsequently triggers the production of fibroblast growth factor 15 (FGF15). FGF15 is then released into the portal vein and carried to the liver, where it forms a crucial interaction with the fibroblast growth factor receptor 4 (FGFR4). This interaction has a significant effect, leading to the inhibition of hepatic BAs biosynthesis from cholesterol (Uriarte et al., 2013). By inhibiting FXR and FGF15 in this pathway, it can alleviate their inhibitory effects on cholesterol degradation, thereby promoting the conversion of cholesterol into BAs. The oxidation products of phenolic compounds in natural foods such as theabrownin inhibited the intestinal FXR-FGF15 signaling pathway, thus reducing hepatic cholesterol. While in the liver, FXR serves as a BAs receptor, which shifts BAs biosynthesis from the classical pathway to the alternative pathway (Jia et al., 2021). Besides, the changes in BA pools and compositions impact cholesterol metabolism due to the FXR-agonistic or antagonistic potencies (Ling et al., 2019). Previous studies have indicated that natural sources abundant in phenolic compounds and their oxidation products, such as green tea and black tea, demonstrated similar cholesterol-lowering effects and altered the BAs metabolism by FXR-FGF15 signaling (Pan et al., 2016; Liu et al., 2022c). However, there is rare research on the function of bioactive substances

in BLR on FXR-FGF15 signaling and the differences with LR in the regulation of cholesterol metabolism.

Therefore, the objectives of the present study were to (i) identify the main bioactive compounds in LR and BLR. (ii) investigate and compare the effects of LR extract and BLR extract on cholesterol metabolism; (iii) explore impacts of LR extract and BLR extract on the gut microbiota of HFD-fed mice. This study will provide new insight into utilizing BLR and essential data that support the bioactive compounds in LR and BLR on modulating cholesterol metabolism.

2. Materials and methods

2.1. Materials and chemicals

Fresh LRs (*Nelumbo.nueifera* cv. 'Honghuhonglian') were obtained from a local market in Honghu (Hubei, China). All standards were obtained from Sigma-Aldrich (St. Louis, MO, USA). All antibodies were purchased from Abcam (Cambridge, MA, USA). Folin-Ciocalteu reagent, HPLC-grade acetonitrile, methanol, formic acid, isopropanol, and BAs were obtained from Merck (Darmstadt, Germany). Other chemical reagents were analytical grade purchased from Xilong Scientific (Guangdong, China).

2.2. Preparation of BLR slices

LR slices (0.3–0.5 cm thick) were placed in a constant temperature and humidity incubator (HPX-160BSH, Shanghai Xinmiao Device Manufacturing Co., Ltd, Shanghai, China) at 20 °C until completely brown for 3 d. Before using the constant temperature and humidity incubator, ultraviolet sterilization was performed to keep the browning environment clean and avoid the deterioration of LR. The BLR slices were freeze-dried and stored at –20 °C (Jiang et al., 2012).

The surface color of LR slices was measured with a chromameter (CR-10, Konica Minolta, Osaka, Japan) (Liao et al., 2020). CIE L*, a*, and b* values represent light-dark, red-green, and yellow-blue coordinates. BI values were measured daily during the browning storage. The browning index (BI) was calculated according to the equations:

$$BI = [100(x-0.31)]/0.172,$$

$$\text{where } x = (a + 1.75L)/(5.645L + a - 3.012b).$$

2.3. Sample preparation

Freeze-dried LR and BLR slices were ground into powder and through a 100-mesh sieve. The dried powder (500 g) of LR or BLR was separately extracted by 1 L of 80% ethanol for 30 min by ultrasonication (Greenapple, Shanghai, China). A Sorvall SL16 centrifuge was used to centrifuge the extract for 10 min at 4200 rpm (Thermo Scientific, Waltham, MA, USA). The residue was twice extracted after the supernatant was separated. The supernatants were combined and rotationally evaporated at 45 °C. The obtained paste was freeze-dried and stored at –20 °C.

2.4. Determination of total phenolic and flavonoid contents

The TPC was determined by using the Folin-Ciocalteu method (Sun et al., 2013). The absorbance was measured at 760 nm. The TPC was calculated using the calibration curves for gallic acid (0–100 $\mu\text{g/mL}$; $r^2 = 0.9993$) and represented as milligrams of gallic acid equivalents per gram of dry weight sample (mg GAE/g DW). The total flavonoid contents (TFC) of the LR extract or BLR extract were determined by the method of Sun et al. (2015). The absorbance was measured at 510 nm. The catechin was used as an equivalent (0–60 $\mu\text{g/mL}$; $r^2 = 0.9997$). It was represented as mg of catechin equivalents per gram of dry weight (mg CAE/g DW).

2.5. Antioxidant activity of LR and BLR

The 2,2'-azinobis-(3-ethylbenzthiazolin-6-sulphonate) (ABTS), 2,2-diphenyl-1-picrylhydrazyl (DPPH) radical scavenging activity and ferric reducing antioxidant power (FRAP) were tested according to previous studies (Mareček et al., 2017; Li et al., 2019). Briefly, 175 μ L of ABTS radical cation combined with 25 μ L of sample were reacted for 6 min. The absorbance of the mixture was measured at 405 nm. For DPPH radical scavenging activity, 100 μ L of newly made DPPH solution combined with 20 μ L of sample were reacted for 30 min in darkness. The absorbance of the mixture was detected at 515 nm. Data were expressed as Trolox equivalent per gram of dried weight sample (mmol Trolox/g DW). For FRAP, 180 μ L of FRAP reagent combined with 20 μ L of sample were reacted for 30 min. The absorbance was measured at 595 nm. Data were reported as FeSO₄ equivalent per gram of dried weight sample (μ mol FeSO₄/g DW).

2.6. Qualitative and quantitative analysis of LR extract and BLR extract

An Agilent 1290 UPLC system (Agilent Technologies, Santa Clara, CA, USA) was used to analyze the extracts, which linked with an Agilent 6538 Accurate-Mass quadrupole time-of-flight mass spectrometer (Agilent Technologies, Santa Clara, CA, USA). The Agilent Zorbax Eclipse Plus-C18 column (4.6 mm \times 250 mm, 5 μ m) was used to analyze. The 0.1% formic acid in water (solvent A) and methanol (solvent B) constituted the binary mobile phase. The gradient elution program was as follows: 0–5 min, 5%–65% B, 15–25 min, 65%–100% B, 25–30 min, 100% B. The flow rate was 0.3 mL/min, and the sample injection volume was 3 μ L. The UV absorbance was detected at 280 nm. The MS/MS parameters were as follows: the orthogonal electrospray ionization (ESI) source; negative ion mode; fragmentor voltage, 135 V; capillary voltage, +4.0 kV; collision gas, nitrogen; collision energy, 20 eV; scan mode, multiple reaction monitoring (MRM). Full scan mass spectrum data were recorded across a range from m/z 50 to 900. MassHunter Acquisition B.03.01 was used to analyze.

Quantitative analysis was performed by UPLC-ESI-QqQ-MS/MS. The Agilent 1290 UPLC system connected with an Agilent 6430 triple quadrupole mass spectrometer LC/MS system (Agilent Technologies, Santa Clara, CA, USA) was performed to quantify. The conditions were same as qualitative analysis. The bioactive compounds in LR or BLR extract were quantified using the calibration curves.

2.7. Animals and diets

All animal procedures and testing were performed in compliance with the National legislation on the use and care of laboratory animals and were approved by the Experimental Animals Ethics Committee of Nanchang University (Permit Number: 0064257). A total of 72 C57BL/6J male mice (8-weeks old) were purchased from Charles River Laboratory Animal Technology Co., Ltd. (Beijing, China). All mice were raised under controllable conditions, a 12 h light/dark cycle at 20–22 °C and 45 \pm 5% humidity. Mice were acclimatized and fed a commercial standard diet for 1 week. A total of 72 C57BL/6J male mice were randomly divided into 9 groups (n = 8): (1) normal diet (ND), (2) high-fat diet (HFD), (3) HFD with LR extract at a low dose of 100 mg/kg/day (HFD + LL), (4) HFD with LR extract at a medium dose of 400 mg/kg/day (HFD + LM), (5) HFD with LR extract at a high dose of 1200 mg/kg/day (HFD + LH), (6) HFD with BLR extract at a low dose of 100 mg/kg/day (HFD + BL), (7) HFD with BLR extract at a medium dose of 400 mg/kg/day (HFD + BM), (8) HFD with BLR extract at a high dose of 1200 mg/kg/day (HFD + BH), (9) HFD with positive control (Xuezhikang Capsule (XZK)) at a dose of 100 mg/kg/day (HFD + XZK). A daily dose of 100 mg/kg/day/mouse was estimated as 487.80 mg/day of LR extract or BLR extract for a 60 kg human (human equivalent dose (mg/kg) = animal dose (mg/kg) \times K_m ratio). The correction factor (K_m) is estimated by dividing the average body weight (kg) of species to its body surface

area (m²) (Nair & Jacob, 2016). Both the ND and HFD were produced by Nanjing Shengmin Scientific Research Animal Farm (Nanjing, China), and the compositions are shown in Supplementary Table 1. The LR extract, BLR extract, and XZK were dissolved in saline, while the ND and HFD groups received saline as controls. All mice were treated orally by gavage once a day. The food and water were available ad libitum. Body weights and food intake were recorded once every 3 days. After 6 weeks of intervention, mice were fasted overnight before being euthanized. Blood samples were collected and then kept at room temperature for half an hour to ensure complete clotting before centrifugation at 4 °C, 5000 rpm for 10 min to obtain the serum sample. The liver, epididymal white adipose tissue (eWAT), perirenal fat, and ileum were weighed and stored at –80 °C for analysis. Besides, the cecal contents were collected and stored at –80 °C.

2.8. Morphology of liver tissue

Hepatic tissues were fixed with 4% paraformaldehyde and embedded in paraffin. The 5 μ m sections were prepared and stained with hematoxylin and eosin (H&E). The physiology of hepatic tissues was visualized using an inverted microscope (Olympus, Tokyo, Japan) under a magnification of 200 \times .

2.9. Analysis of hepatic and fecal BAs

Each 50 mg of hepatic or fecal samples was extracted with 200 mL of methanol/water (1:1, v/v) using ultra-sonication for 30 min. The 18 types of BAs were quantified using standard curves (Chen et al., 2020). BA concentrations were tested using UPLC-ESI-QTOF-MS/MS (Waters Corp., Milford, MA, USA) equipped with ACQUITY HSS T3 column (2.1 \times 100 mm, 1.8 μ m, Waters Corp., Milford, MA, USA). In the binary mobile phase, the solvents A and B were 0.1% ammonium acetate in water/acetonitrile (10/1, v/v) and acetonitrile/isopropanol solution (1/1, v/v). The gradient program was as follows: 0–6 min, 0%–45% B; 7–9 min, 45%–60% B; 9–12 min, 60%–100% B; 12–13 min, 100%–0% B. The flow rate was 0.3 mL/min. The sample injection volume was 3 μ L. The condition of 5500 Qtrap mass spectrometer (AB SCIEX, Foster City, CA, USA) was used to get the MS spectrum: the ESI source in the negative ion mode; scan mode, MRM; capillary voltage, 2.00 kV. The BAs were quantified using the TargetLynx application manager.

2.10. Measurement of biochemical indicators

The contents of total cholesterol (TC), triglycerides (TG), low-density lipoprotein-cholesterol (LDL-C), high-density lipoprotein-cholesterol (HDL-C), apical sodium-dependent bile acid transporter (ABST), ileal bile acid-binding protein (IBABP), and FXR were quantified according to the instruction of commercial kits (Nanjing Jiancheng Bioengineering Institute, Nanjing, China).

2.11. Quantitative real-time polymerase chain reaction (qRT-PCR)

The qRT-PCR was determined with TB Green™ Premix Ex Taq™ (Tli RNaseH Plus, Takara BIO, Shiga, Japan). RNA was reverse transcribed into cDNA using a Prime Script RT reagent kit (Takara, Japan). All procedures were carried out under the manufacturer's instruction. The mRNA level was quantified by the $\Delta\Delta$ Ct method. GAPDH was used as the housekeeping gene and relative expression level was shown as fold changes relative to the ND group. The forward and reverse sequences of qPCR primers are shown in Supplementary Table 2.

2.12. Western blot

The total protein was extracted using RIPA buffer for 30 min. The extracted protein was separated by 10% SDS-PAGE, and then transferred to polyvinylidene difluoride (PVDF) membranes. The membranes were

incubated with primary antibodies and secondary antibodies. The bands were visualized with an imaging system (Bio-Rad, Hercules, CA, USA). GAPDH was the internal reference. The antibody dilutions are shown in [Supplementary Table 3](#).

2.13. Gut microbe 16S rRNA sequencing

According to manufacturer instructions, the Microbial genome DNA was extracted from cecal contents with the Magnetic Soil And Stool DNA Kit (Tiangen Biotech Co., Ltd., Beijing, China). The DNA concentration was determined using the Qubit dsDNA HS Assay Kit and Qubit 3.0 Fluorometer (Invitrogen, Thermo Fisher Scientific, Oregon, USA). The full-length 16S rRNA gene was amplified from genomic DNA extracted from each sample using a universal primer set, the 27F: AGRGTTGATYNTGGCTCAG and 1492R: TASGGHTACCTTGTTASGACTT. The PCR conditions were as follows: 25 cycles of PCR amplification with denaturation at 95 °C for 2 min, annealing at 55 °C for 30 s, elongation at 72 °C for 1 min and 30 s, and a final step at 72 °C for 10 min. The total of PCR amplicons was purified with Agencourt AMPure XP Beads (Beckman Coulter, Indianapolis, USA). The purified PCR products were quantified using the Qubit dsDNA HS Assay Kit and Qubit 3.0 Fluorometer (Invitrogen, Thermo Fisher Scientific, Oregon, USA). SMRTbell libraries from the pooled and barcoded samples were sequenced on a single PacBio Sequel II 8M cell using the Sequel II Sequencing Kit 2.0. The bioinformatics analysis of this study was performed with the aid of the BMK Cloud (Biomarker Technologies Co., Ltd, China).

2.14. Statistical analysis

All data were presented as mean \pm SEM (standard error of the mean,

$n = 8$ individuals/group). Statistical analysis was performed using SPSS software (Version 25.0, SPSS Inc., Chicago, IL, USA). Graph bars marked with different letters on top represent statistically significant results ($P < 0.05$) based on One-way ANOVA analysis followed by Duncan's test, whereas bars labelled with the same letter correspond to results that show no statistically significant differences. When two letters are present on top of the bar, each letter should be compared separately with the letters of other bars to determine whether the results show statistically significant differences.

3. Results and discussion

3.1. Changes of LR before and after browning

The color change of LR slices was presented in [Fig. 1A](#) (a: complete LR, b: LR slice, c: BLR slice). During storage at 20 °C, the BI and L^* , a^* , and b^* of LR slices increased gradually and did not change significantly until day 3. Thus, the browning time of LR slices was 3 days, and the BI value of LR stored at 20 °C on day 3 reached 81.52. Furthermore, there was a noticeable increase in the TPC and TFC levels in completely browned BLR slices when compared to those in fresh LR slices ($P < 0.01$). In detail, the TPC was 4.89 ± 0.13 mg GAE/g DW for fresh LR slices and 8.89 ± 0.23 mg GAE/g DW for completely BLR slices ([Fig. 1C](#)). The TFC was 4.83 ± 0.10 mg CAE/g DW for fresh LR slices and 10.29 ± 0.19 mg CAE/g DW for completely BLR slices ([Fig. 1D](#)). Previous studies have confirmed similar results ([Min et al., 2017](#)). The ABTS, DPPH radical-scavenging activities, and the antioxidant activity of FRAP assay of BLR extract were more effective than LR extract ([Fig. 1E, F, G](#)). It was speculated that the compounds produced during the storage and browning period had more substantial antioxidant capacity.

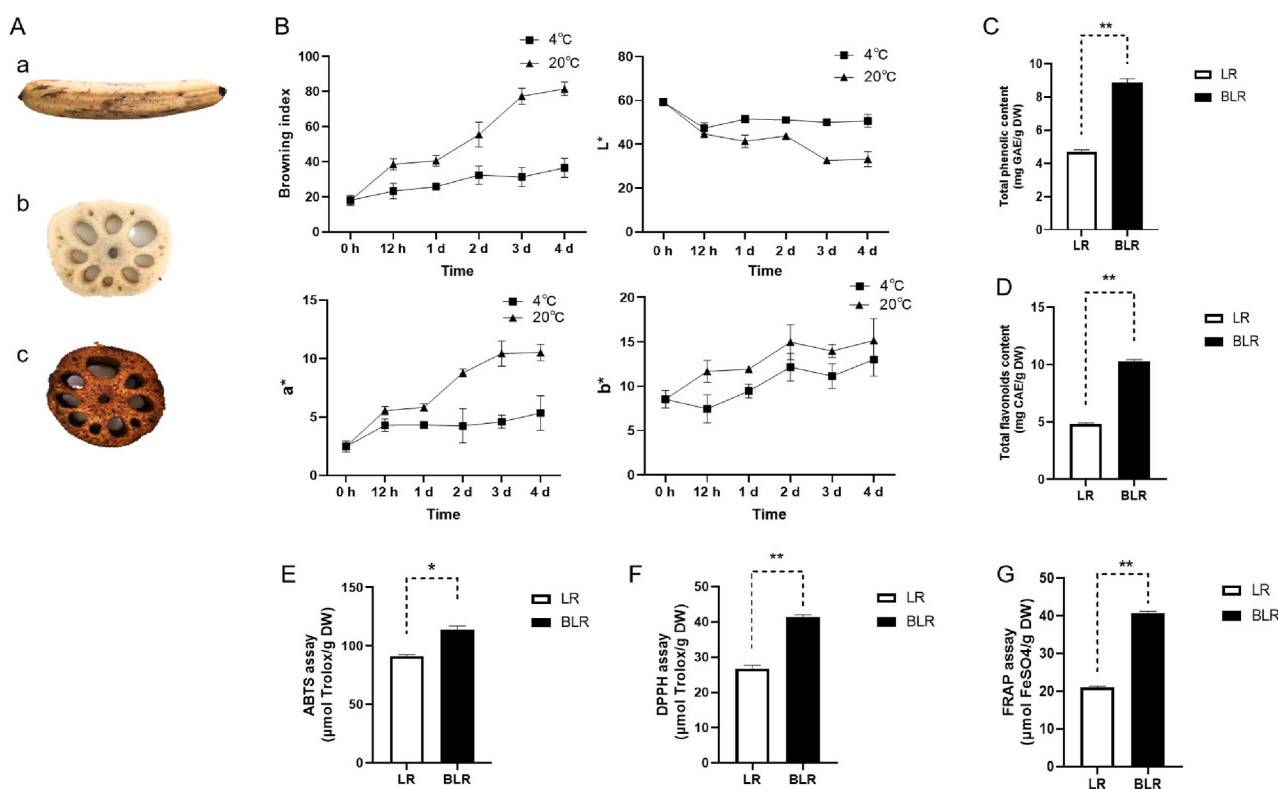


Fig. 1. Changes of lotus root (LR) before and after the browning storage. A. Pictures of LR before and after browning storage. a. fresh complete lotus root; b. fresh lotus root slices; c. browning lotus root (BLR) slices at 20 °C; B. Browning index of LR slices. Chromaticity L^* represents light-dark; a^* represents red-green; b^* represents yellow-blue; C. Total phenolic content in LR and BLR; D. Total flavonoids content in LR and BLR; E. The ABTS radical-scavenging activities in LR and BLR; F. The DPPH radical-scavenging activities in LR and BLR; G. The antioxidant activity of FRAP assay in LR and BLR. * $p < 0.05$, ** $p < 0.01$ by the student's t -test indicates significant differences between the LR and BLR groups. (For interpretation of the references to color in this figure legend, the reader is referred to the Web version of this article.)

3.2. Qualitative and quantitative analysis of LR extract and BLR extract

A total of 17 bioactive compounds were identified in the LR extract and 14 compounds in the BLR extract (Table 1). Specifically, Peak 1 was identified as chlorogenic acid based on the molecular ion $[M-H]^-$ at m/z 353.0901 and the fragment ion at m/z 191.0379 ($[\text{quinic acid-H}]^-$) (Li et al., 2019). Peak 2 was identified as gluconic acid according to the previous study (Sun et al., 2017). Peak 3 was identified as caffeic acid based on the molecular ion $[M-H]^-$ at m/z 179.0357 by matching its MS data of the authentic standard and previous literature (La et al., 2015). Peak 4 was suggested as malic acid according to Sun et al. (2015). Peak 5 was tentatively assigned as caffeic acid hexose and confirmed by the MS/MS fragment ion at m/z 179.0565 (Ye et al., 2015). Peaks 6 with precursor ions $[M-H]^-$ at m/z 337.0929 was identified as 5-*p*-coumaroylquinic acid (Li et al., 2019). Peak 7 ($[M-H]^-$ at m/z 173.0452) was assigned as shikimic acid based on the MS data of the standard and literature (Shukla et al., 2021). Peak 8 was identified as quinic acid by comparing its precursor ion $[M-H]^-$ at m/z 191.0554 with the MS data of the standard (Li et al., 2019). Peak 9 with the precursor ion $[M-H]^-$ at m/z 180.0684 was tentatively presented as tyrosine (Fraser et al., 2014). Peak 10 was identified as succinic acid by comparing it with the MS data of the standard (Sun et al., 2017). Peak 12, with a molecular ion $[M-H]^-$ at m/z 305.0675 and MS/MS fragment ion at m/z 261.0775 $[M-H-CO]^-$ (catechin moiety), was identified as epigallocatechin (Cao et al., 2018). Similarly, Peak 11 with the precursor ion $[M-H]^-$ at m/z 609.1264 was tentatively identified as epigallocatechin dimer, since the fragment ion at m/z 305.0670 was consistent with epigallocatechin. Peak 13 was identified as procyanidin B1 according to the molecular ion $[M-H]^-$ at m/z 577.1369 and the major fragments (Zhang et al., 2022b). Peak 14 and 15 were identified as catechin and epicatechin respectively based on their MS/MS data and t_R of the authentic standard and previous literature (Zhang et al., 2022b). Naringenin was detected in Peak 16 based on the MS data of the authentic standard and previous literature (Santos et al., 2011). Peak 17 with the molecular ion $[M-H]^-$ at m/z 455.3549 was identified as betulinic acid (Moreno-González et al., 2020).

Peaks 18–21 were the main compounds identified in the BLR extract. Peak 18, with a molecular ion $[M-H]^-$ at m/z 451.1273 and the major fragments at m/z 289.0716 (catechin moiety), was identified as

catechin-7-*O*-glucoside (Ojwang et al., 2013). Peak 19 was identified as forsythoside A based on a molecular ion $[M-H]^-$ at m/z 623.1985, as well as the major fragment at m/z 460.1771 resulting from the loss of the caffeoyl moiety $[M-H-162]^-$ (Marchetti et al., 2019). Based on the study of Liu et al. (2022b) and the t_R , MS, and MS/MS data of the authentic standards, Peak 20 was assigned as theaflavin ($[M-H]^-$ at m/z 563.1199). Peak 21 was identified as adenosine by comparing with MS data (molecular ion $[M-H]^-$ at m/z 266.0893) of the authentic standard.

Table 2 shows that the main bioactive compound with the highest content in LR extract was catechin ($325.14 \pm 0.09 \mu\text{g/g DW}$), followed by quinic acid ($237.36 \pm 18.92 \mu\text{g/g DW}$), epigallocatechin ($99.53 \pm 13.65 \mu\text{g/g DW}$). Compared with LR, theaflavin ($117.89 \pm 14.04 \mu\text{g/g DW}$), forsythoside A ($76.20 \pm 7.66 \mu\text{g/g DW}$), adenosine ($35.62 \pm 3.11 \mu\text{g/g DW}$), and catechin-7-*O*-glucoside ($15.36 \pm 0.19 \mu\text{g/g DW}$) were newly detected in BLR. Most notably, the contents of catechin and epigallocatechin decreased remarkably while the content of theaflavin increased dramatically in BLR, which indicated a large amount of catechins were oxidized to theaflavin. Theaflavin is generated via the successive oxidation of catechins by PPO. Zhang et al. (2020) used a mixture of catechins like catechin and epigallocatechin as substrates to conduct theaflavin via PPO catalytic oxidation. Jin et al. (2013) revealed theaflavin is a functional component that contributed to the decreased TC in HFD rats. The newly formed forsythoside A in BLR is a kind of caffeic acid derivative, which was a phenylethanoid glycoside with one caffeic acyl group. Forsythoside A showed an anti-inflammatory effect on LPS-induced acute lung injury (Liu et al., 2022a). The catechin-7-*O*-glucoside was formed by the glycosylation of catechin. The effects of catechin glycosylation include increasing water solubility and enhancing the in-vivo stability and bioavailability of catechin. The adenosine found in BLR, a nucleoside composed of adenine and D-ribose, is used to treat chronic heart failure and aids in the protection of the cardioprotective circulatory system (Iamtham et al., 2022). Sun et al. (2018) detected that the contents of adenosine in the leftovers of LR from different places were 0–0.103 $\mu\text{g/g}$. In our present study, LR was mechanically damaged during slicing, and as the plant cells ruptured and cytoplasmic leaching during browning storage, allowing the adenosine to be detected in BLR. The content of naringenin in BLR was increased, which is the first stable intermediate product in the flavonoid

Table 1
Qualitative analysis of bioactive compounds in LR extract and BLR extract.

Peak no.	t_R (min)	Formula	(M-H)-			Major fragment ions (m/z)	Proposed compounds	Found in LR or BLR
			Measured	Calculated	Error (ppm)			
1	3.343	C ₁₆ H ₁₈ O ₉	353.0901	353.0878	6.5	165.0406, 191.0379	Chlorogenic acid ^{a,b,c}	LR
2	3.454	C ₆ H ₁₂ O ₇	195.0513	195.051	1.4	59.0139, 75.0089	Gluconic acid ^{b,c}	LR, BLR
3	3.57	C ₉ H ₈ O ₄	179.0357	179.035	4.01	75.009	Caffeic acid ^{a,b,c}	LR, BLR
4	4.251	C ₄ H ₆ O ₅	133.0148	133.0142	4.16	71.0142, 115.0036	Malic acid ^{b,c}	LR, BLR
5	4.476	C ₁₅ H ₁₈ O ₉	341.0878	341.0878	-0.02	59.0140, 179.0565	Caffeic acid hexose ^{b,c}	LR
6	4.738	C ₁₆ H ₁₈ O ₈	337.073	337.0929	0.32	190.5793	5- <i>p</i> -Coumaroylquinic acid ^{a,b,c}	LR
7	4.816	C ₇ H ₁₀ O ₅	173.0452	173.0455	-2.01	55.0193, 71.0142	Shikimic acid ^{a,b,c}	LR
8	5.5	C ₇ H ₁₂ O ₆	191.0554	191.0561	-3.74	87.0088, 111.0087	Quinic acid ^{a,b,c}	LR, BLR
9	6.181	C ₉ H ₁₁ NO ₃	180.0684	180.0666	9.84	119.0503, 163.0399	Tyrosine ^{b,c}	LR, BLR
10	6.406	C ₄ H ₆ O ₄	117.0197	117.0193	3.14	73.0295, 99.0087	Succinic acid ^{a,b,c}	LR, BLR
11	6.863	C ₃₀ H ₂₆ O ₁₄	609.1264	609.125	2.33	305.067	Epigallocatechin dimer ^{a,b,c}	LR
12	9.02	C ₁₅ H ₁₄ O ₇	305.0675	305.0667	0.6	125.0246, 261.0775	Epigallocatechin ^{a,b,c}	LR
13	10.156	C ₃₀ H ₂₆ O ₁₂	577.1369	577.1351	3.03	289.0724, 407.0779	Procyanidin B1 ^{a,b,c}	LR
14	11.974	C ₁₅ H ₁₄ O ₆	289.073	289.0723	2.5	109.0295, 245.0825, 271.0612	Catechin ^{a,b,c}	LR, BLR
15	14.134	C ₁₅ H ₁₄ O ₆	289.0724	289.0723	2.21	109.0283, 125.0232, 151.0392, 203.0707, 245.0817	Epicatechin ^{a,b,c}	LR, BLR
16	22.916	C ₁₅ H ₁₂ O ₅	271.0612	271.0612	0	107.0140, 119.9468, 125.0224, 197.0607	Naringenin ^{a,b,c}	LR, BLR
17	29.469	C ₃₀ H ₄₈ O ₃	455.3549	455.3531	4.02	112.9859, 135.8063, 311.1698	Betulinic acid ^{a,b,c}	LR, BLR
18	10.526	C ₂₁ H ₂₄ O ₁₁	451.1273	451.1246	6.02	289.0716	Catechin-7- <i>O</i> -glucoside ^{b,c}	BLR
19	22.694	C ₂₉ H ₃₆ O ₁₅	623.1985	623.1981	0.57	179.0561, 297.1137, 460.1771	Forsythoside A ^{a,b,c}	BLR
20	22.879	C ₂₉ H ₂₄ O ₁₂	563.1199	563.1195	0.71	137.0244, 400.1562, 401.1588, 426.1333	Theaflavin ^{a,b,c}	BLR
21	23.107	C ₁₀ H ₁₃ N ₅ O ₄	266.0893	266.0895	-0.67	119.0499, 134.0610, 146.0412	Adenosine ^{a,b,c}	BLR

Note: ^a Compared with standard. ^b Compared with MSⁿ data or/and data bases. ^c Compared with the literatures.

Table 2

The quantitative analysis of main bioactive compounds in LR extract and BLR extract.

Peak no.	Compounds	LR ($\mu\text{g/g DW}$)	BLR ($\mu\text{g/g DW}$)	Calibration curve equation	R2	Range ($\mu\text{g/mL}$)
1	Chlorogenic acid	41.96 \pm 5.21	16.44 \pm 2.81	y = 24.145x+14.35	0.9997	1–200
3	Caffeic acid	42.00 \pm 3.95	5.23 \pm 0.51	y = 94.589x+408.61	0.9991	1–200
6	5-p-Coumaroylquinic acid	9.08 \pm 0.63	ND	y = 20.196x+6.87	0.9987	0.2–40
8	Quinic acid	237.36 \pm 18.92	234.87 \pm 0.60	y = 268.02x+318.96	0.999	2–400
11	Epigallocatechin dimer	52.45 \pm 6.69	ND	y = 322.25x+200.12	0.9992	1–200
12	Epigallocatechin	99.53 \pm 13.65	ND	y = 322.25x+200.12	0.9992	1–200
13	Procyanidin B1	12.78 \pm 0.85	ND	y = 65.227x+6.153	0.9989	0.2–40
14	Catechin	325.14 \pm 0.09	6.66 \pm 0.88	y = 64.875x+242.24	0.9992	1–200
15	Epicatechin	8.50 \pm 1.81	0.53 \pm 0.01	y = 72.104x+34.173	0.9991	0.2–40
16	Naringenin	8.02 \pm 0.73	11.38 \pm 1.06	y = 168.5x-17.181	0.9996	0.5–20
17	Betulinic acid	81.97 \pm 2.47	60.26 \pm 6.47	y = 269.61x+420.59	0.9991	1–200
18	Catechin-7-O-glucoside	ND	15.36 \pm 0.19	y = 64.875x+242.24	0.9992	1–200
19	Forsythoside A	ND	76.20 \pm 7.66	y = 94.589x+408.61	0.9991	1–200
20	Theaflavin	ND	117.89 \pm 14.04	y = 6.958x-2.6709	0.999	1.15–230
21	Adenosine	ND	35.62 \pm 3.11	y = 29.51x+11.628	0.9992	0.5–40

Note: All data in the table are shown as mean \pm SEM.

synthesis pathway (Liu et al., 2022b). The contents of quinic acid in LR and BLR were slightly different, which may be due to the fact that quinic acid did not contain phenolic hydroxyl and can not be oxidized by PPO.

3.3. Body weight, food intake and adipose tissue

The trend of body weight of mice is shown in Fig. 2 A. All groups had similar initial body weights (from 20.13 \pm 0.70g to 20.34 \pm 0.51 g, $P > 0.05$), while the final body weight of mice in the HFD group (30.79 \pm 0.83 g) was significantly higher than that in the ND group (25.38 \pm 0.54 g, $P < 0.05$). Compared with the HFD group, all doses of LR extract and BLR extract, including low (LL and BL), medium (LM and BM), and high doses (LH and BH), significantly reduced the body weight of mice with a dose-dependent effect ($P < 0.05$). There was no significant difference between the daily food intake of the ND group and other 8 groups (Table 3, 3.30–3.60 g/day/mouse, $P > 0.05$), inferring that the weight losses induced by LR extract or BLR extract were not due to the reduction of food intake. The low, medium, and high doses of LR extract and BLR extract significantly reduced the weight of eWAT and perirenal fat compared to the HFD group (Table 3, $P < 0.05$). Notably, the weight of eWAT in the consumption of BLR extract (0.31 \pm 0.02 g, 0.26 \pm 0.02 g, 0.24 \pm 0.01 g in HFD + BL, HFD + BM, HFD + BH, respectively) was significantly lower than that of LR extract (0.76 \pm 0.04 g, 0.41 \pm 0.01 g, 0.30 \pm 0.01 g in HFD + LL, HFD + LM, HFD + LH) at the same dose ($P < 0.05$). The results implied a potential inhibitory effect of BLR extract on the eWAT weight. Both LR extract and BLR extract significantly reduced liver weight compared with the HFD group, and BLR extract consumption at the high dose (HFD + BH) has the most obvious effect on liver weight (Table 3, $P < 0.05$).

In particular, BLR extract was superior to LR extract in terms of lowering eWAT weight (Table 3, $P < 0.05$). These differences may be caused by the different main components in LR extract and BLR extract. The content of catechin was the highest in LR extract while its content in BLR extract decreased sharply, and theaflavin, as the oxidation product of catechin, was the newly generated bioactive compound with the highest content in BLR extract. Liu et al. (2022c) confirmed that the intake of oxidized tea phenolics rich in theaflavins effectively suppressed the accumulation of eWAT compared with the HFD group, and the suppression was even better than that of catechins-rich green tea. Similarly, the high theaflavin content in BLR extract, resulting from the oxidation process, may explain its superior performance in reducing eWAT weight compared to LR extract. This connection between theaflavin and their enhanced impact on eWAT reduction underpinned our findings and highlighted the potential health benefits of the bioactive compounds in BLR extract.

3.4. Hepatic and serum lipid- and cholesterol-lowering effects of LR and BLR extract

HFD induced the elevation of hepatic TC and TG, while the levels of TC were reduced significantly with the treatment of LR extract or BLR extract compared with that of HFD group (Fig. 2 B, $P < 0.05$). BLR extract at 1200 mg/kg/day (high dose) was the most effective in reducing TC. In the groups of LR extract or BLR extract consumption at medium and high doses, the levels of hepatic TG were all significantly lower than that of the HFD group (Fig. 2 C, $P < 0.05$). Similar results were also found in the serum (Fig. 2 G, H). BLR extract at high dose was the most effective in reducing serum TC. Furthermore, it was observed that even a low dose of BLR extract significantly reduced the serum TG levels in HFD-fed mice. The LDL-C/HDL-C ratio is recognized as an accurate predictor of several unfavorable cardiovascular events (Du et al., 2020). The level of hepatic LDL-C increased and HDL-C decreased due to the HFD (Fig. 2 D, E, F). After LR extract or BLR extract gavage for six weeks, the LDL-C levels were significantly decreased in HFD + LM, HFD + LH, HFD + BM, and HFD + BH groups ($P < 0.05$). The hepatic HDL-C levels were obviously increased in HFD + LH, HFD + BM, and HFD + BH groups compared with the HFD group ($P < 0.05$). The LDL-C/HDL-C ratio rise induced by HFD was substantially suppressed by either LR extract or BLR extract especially at high dose. In serum, it was observed that both LR extract and BLR extract had a significant impact on increasing HDL-C levels ($P < 0.05$) but did not show a significant effect on reducing LDL-C levels. Nevertheless, both LR extract and BLR extract were effective in significantly reducing the LDL-C/HDL-C ratio (Fig. 2 I, J, K, $P < 0.05$). Previous study also found that the intake of ethanol extract of LR decreased the TC and TG in HFD rats (You et al., 2014). Liu et al. (2022c) confirmed that the effect of theaflavin-rich black tea extract on lowering serum TC was greater than that of catechins-rich green tea extract. Our study further substantiated these findings by confirming the lipid- and cholesterol-lowering properties of LR and BLR. Notably, BLR extract at high dose displayed the most significant reduction in serum TC levels. Building upon these findings, further investigations are warranted to explore their full potential for managing cholesterol metabolism.

3.5. Effects of LR extract and BLR extract on hepatic histology

The hepatocyte steatosis and focal infiltration of hepatic inflammatory cells with H&E staining were clearly observed in the HFD group, which were marked with red and black arrows in Fig. 3, respectively. The intake of LR extract at low dose (HFD + LL) obviously reduced the focal infiltration of inflammatory cells, but there was still considerable hepatocyte steatosis. While the hepatocyte steatosis markedly alleviated with the increase of LR extract dosage, all hepatocytes appeared normal

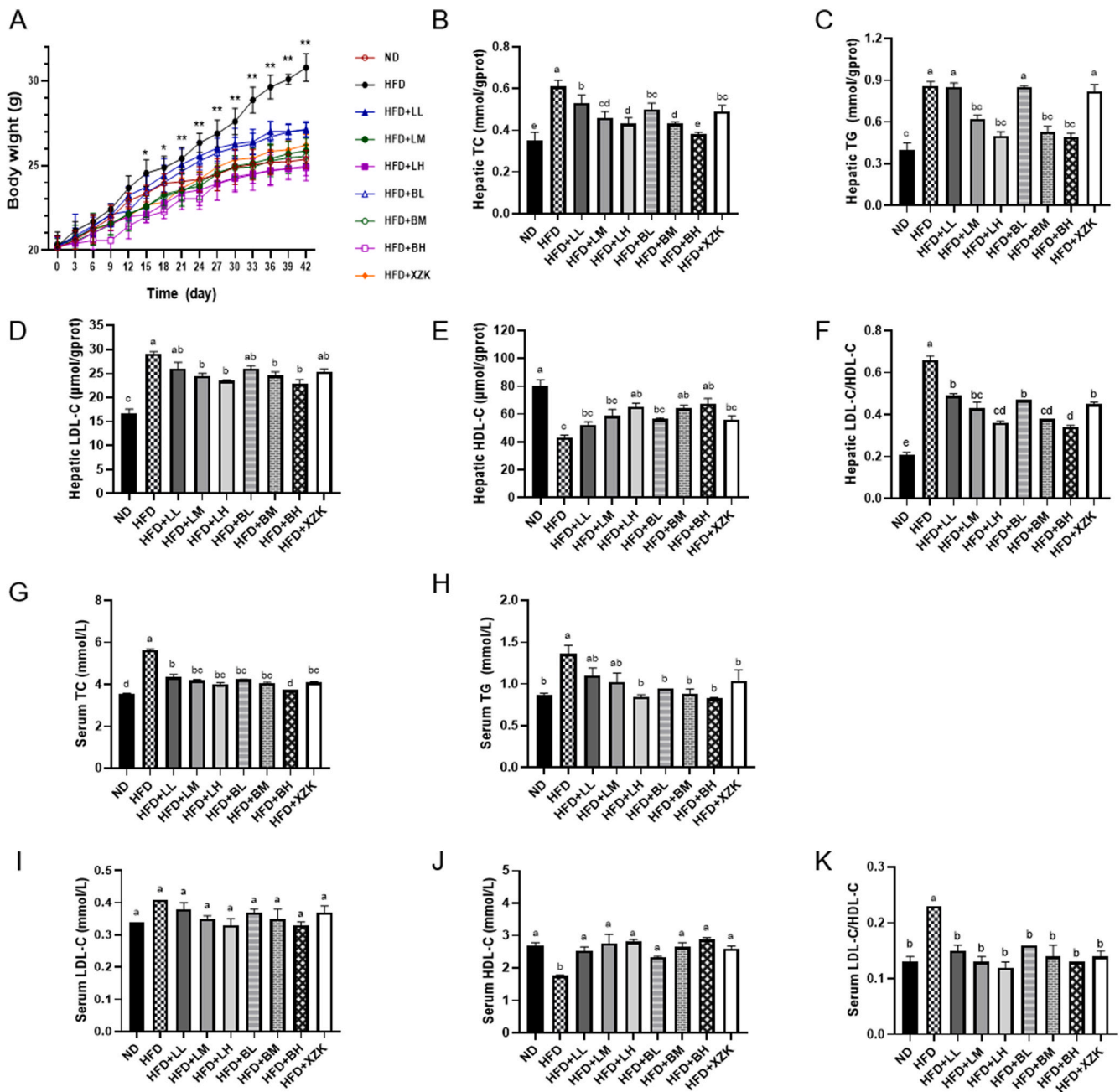


Fig. 2. Changes of body weight and hepatic lipids and cholesterol lowering effects of LR extract and BLR extract on mice. A. Effect of LR extract and BLR extract on body weight increase of mice. * $p < 0.05$, ** $p < 0.01$ by the student's *t*-test indicates significant differences between the HFD and other groups; B. LR extract and BLR extract reduced hepatic total cholesterol (TC) contents of mice with HFD diet; C. LR extract and BLR extract reduced hepatic triacylglycerols contents (TG) of mice with HFD diet; D. The hepatic low-density lipoprotein cholesterol (LDL-C) contents; E. The hepatic high-density lipoprotein cholesterol (HDL-C) contents; F. Hepatic LDL-C/HDL-C. G. LR extract and BLR extract reduced serum TC contents of mice with HFD diet; H. LR extract and BLR extract reduced serum TG of mice with HFD diet; I. The serum LDL-C contents; J. The serum HDL-C contents; K. Serum LDL-C/HDL-C. Bars with various letters differ significantly using one-way ANOVA followed by the Duncan's test, $p < 0.05$.

in the HFD + LH group. It is noteworthy that hepatocyte steatosis visibly reduced in the HFD + BL group, while some focal infiltration of inflammatory cells remained (Fig. 3 B, HFD+BL). Similarly, focal infiltration of inflammatory cells in hepatic tissue recovered a lot when treated with BLR extract at medium dose (HFD+BM), and definitely altered back to their natural state with the intake of BLR extract at high dose (HFD+BH). Similar results have been reported that Que Zui tea rich in polyphenols recovered severe hepatic steatosis caused by HFD (Zhang et al., 2022a). Furthermore, Lin et al. (2007) revealed that theaflavin effectively reduced hepatic lipid accumulation in HFD rats, indicating that theaflavin in BLR may play the key role in regulating liver lipid and

cholesterol metabolism. These observations highlighted the considerable potential of LR extract and BLR extract in addressing liver health and managing metabolic disorders. The ability of LR extract and BLR extract to alleviate hepatic steatosis and reduce hepatic focal infiltration of inflammatory cells underscored their role as potential natural remedies dealing with the disorder of liver cholesterol metabolism and related liver health challenges.

3.6. The contents of BAs in the liver and feces

As shown in Table 4, 13 types of BAs were found in the liver

Table 3
Effects of LR extract and BLR extract on food intake, fat mass and organ weight of mice.

	ND	HFD	HFD+LL	HFD+LM	HFD+LH	HFD+BL	HFD+BM	HFD+BH	HFD+XZK
Initial body weight (g)	20.13 ± 0.70a	20.26 ± 0.83a	20.26 ± 0.52a	20.34 ± 0.51a	20.25 ± 0.55a	20.29 ± 0.59a	20.32 ± 0.37a	20.27 ± 0.50a	20.32 ± 0.55a
Final body weight (g)	25.38 ± 0.54d	30.79 ± 0.83a	27.11 ± 0.43b	25.87 ± 0.75cd	24.96 ± 0.56e	27.15 ± 0.46b	25.56 ± 0.68cd	24.88 ± 0.76e	26.21 ± 0.63c
Body weight gain (g)	5.24 ± 0.83cd	10.53 ± 1.00a	6.85 ± 0.70b	5.53 ± 0.72cd	4.71 ± 0.62d	6.86 ± 0.53b	5.24 ± 0.84cd	4.61 ± 1.14d	5.89 ± 0.98bc
Food intake (g/day)	3.30 ± 0.39a	3.60 ± 0.23a	3.57 ± 0.14a	3.48 ± 0.24a	3.55 ± 0.21a	3.58 ± 0.29a	3.47 ± 0.22a	3.53 ± 0.27a	3.50 ± 0.23a
eWAT weight (g)	0.26 ± 0.01c	0.80 ± 0.03a	0.76 ± 0.04a	0.41 ± 0.01b	0.30 ± 0.01bc	0.29 ± 0.02bc	0.26 ± 0.02c	0.24 ± 0.01c	0.40 ± 0.02b
Perirenal fat weight (g)	0.05 ± 0.00de	0.36 ± 0.06a	0.21 ± 0.06b	0.10 ± 0.01cd	0.07 ± 0.00de	0.15 ± 0.04c	0.06 ± 0.01de	0.04 ± 0.00e	0.11 ± 0.03cd
Liver weight (g)	1.25 ± 0.13b	1.48 ± 0.13a	1.16 ± 0.08bcd	1.13 ± 0.08bcd	1.07 ± 0.13cd	1.14 ± 0.06bcd	1.10 ± 0.06cd	1.04 ± 0.15d	1.18 ± 0.07bc

Note: All data in the table are shown as mean ± SEM (n = 8). Means with different letters in the same row are significantly different using one-way ANOVA followed by the Duncan's test, $P < 0.05$.

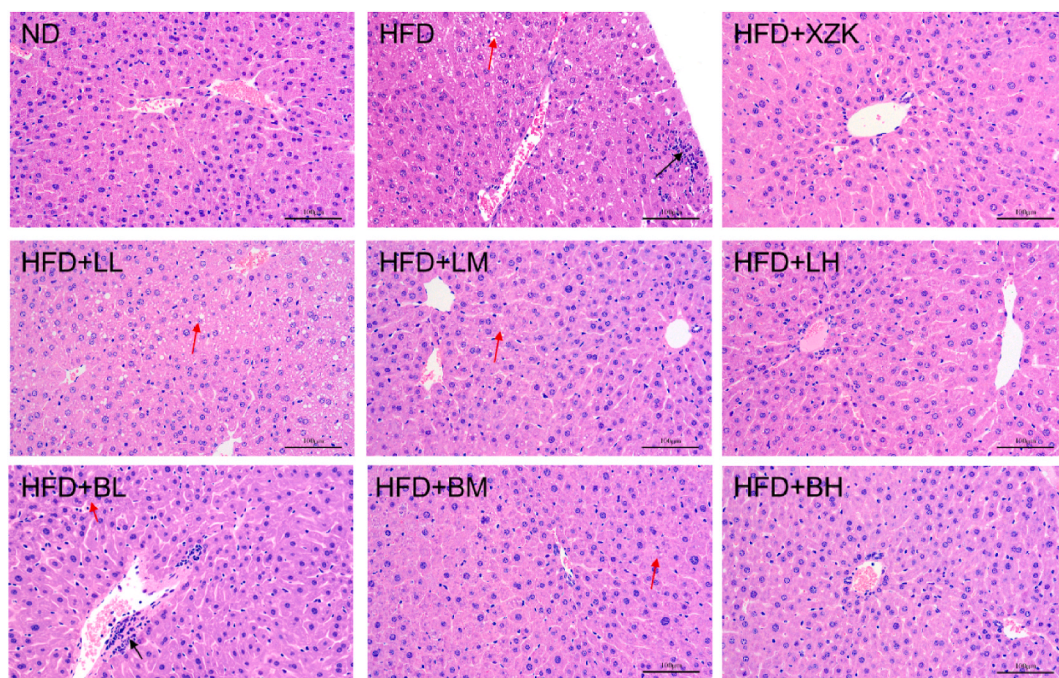


Fig. 3. Effects of LR and BLR extracts on H&E hepatocytes. Red arrows (→) indicated hepatocyte steatosis, and black arrows (→) indicated focal infiltration of hepatic inflammatory cell (200× magnification). (For interpretation of the references to color in this figure legend, the reader is referred to the Web version of this article.)

including 8 primary BAs (P-BAs) and 5 secondary BAs (S-BAs). The total BAs in liver of these five groups, HFD + LH, HFD + BL, HFD + BM, HFD + BH, and HFD + XZK, were significantly higher than HFD group ($P < 0.05$), which indicated that more cholesterol was metabolized into BAs in these groups. In detail, the content of total BAs was 105.26 ± 3.74 ng/mg in the HFD + BH group, which was 2.17 times that of HFD group (48.51 ± 2.32 ng/mg). P-BAs accounted for 92.11%–96.71% of total BAs which made up the majority of BAs in the liver. Furthermore, the TCA and $T(\alpha+\beta)$ MCA accounted for 72.36%–79.85% of the total BAs, which demonstrated that TCA and $T(\alpha+\beta)$ MCA were the most abundant BAs (Sayin et al., 2013). Huang et al. (2019) found that TCA activated hepatic FXR, which inhibited the expression of CYP8B1 in the classical pathway. In the present study, the treatment of BLR extract significantly increased the amount of $T(\alpha+\beta)$ MCA compared to the HFD group ($P < 0.05$). Subsequently, the amount of $T(\alpha+\beta)$ MCA discharged into the intestine also increased. However, only a small amount of $T(\alpha+\beta)$ MCA was excreted in the feces (Table 5), which indicated that most $T(\alpha+\beta)$

MCA were reabsorbed in the ileum. As $T\alpha$ MCA and $T\beta$ MCA are the FXR antagonists (Sayin et al., 2013), most $T(\alpha+\beta)$ MCAs which were reabsorbed may inhibit the ileal FXR gene and protein expressions.

Table 5 shows the content of BAs in the feces of mice including 8 conjugated (C-BAs) and 7 unconjugated (U-BAs) BAs. In HFD+LH, HFD+BM, and HFD+ BH groups, the total content of BAs in feces significantly increased compared to that of the HFD group ($P < 0.05$). And BLR extract improved more significantly BAs excretion in feces than LR extract at the same dose. The findings implied that the intake of BLR extract had a greater potential to promote fecal BA excretion than that of LR extract. The amount of C-BAs in the feces was notably lower than the amount of U-BAs in the feces, suggesting that the majority of the C-BAs were actively reabsorbed into the enterohepatic circulation through the ileum (Chen et al., 2020). Huang et al. (2019) reported similar findings that theabrownin, the oxidative polymerization of catechins, raised ileal C-BAs levels, and inhibited the ileal FXR-FGF15 signaling pathway. These results indicated that C-BAs played a key role in BAs metabolism,

Table 4
Contents of hepatic bile acids after LR extract and BLR extract consumption (ng/mg).

Liver			ND	HFD	HFD+LL	HFD+LM	HFD+LH	HFD+BL	HFD+BM	HFD+BH	HFD+XZK
BA	Source	Structure									
α-MCA	P-BA	U-BA	0.87 ± 0.03de	0.69 ± 0.02e	0.80 ± 0.05de	0.98 ± 0.03d	1.45 ± 0.05c	1.51 ± 0.08c	2.00 ± 0.03b	3.04 ± 0.06a	1.27 ± 0.05c
β-MCA	P-BA	U-BA	3.30 ± 0.19c	2.63 ± 0.14de	2.06 ± 0.14e	2.10 ± 0.12e	3.13 ± 0.10d	4.19 ± 0.20bc	5.31 ± 0.20a	5.02 ± 0.24	3.27 ± 0.21cd
CA	P-BA	U-BA	0.17 ± 0.01e	3.14 ± 0.12bc	2.58 ± 0.11c	2.11 ± 0.09cd	3.54 ± 0.11	3.33 ± 0.12 ab	2.58 ± 0.09c	3.36 ± 0.13	2.28 ± 0.12cd
CDCA	P-BA	U-BA	0.08 ± 0.02e	2.19 ± 0.11d	3.18 ± 0.13bc	2.78 ± 0.05c	3.82 ± 0.12b	3.23 ± 0.12bc	4.20 ± 0.11a	4.34 ± 0.14a	3.13 ± 0.09bc
DHCA	P-BA	U-BA	ND	ND	ND	ND	ND	ND	ND	ND	ND
TCA	P-BA	T-BA	16.18 ± 1.06d	24.42 ± 1.82bcd	20.35 ± 2.20cd	24.99 ± 1.65bcd	30.25 ± 2.47bc	32.96 ± 1.42b	44.49 ± 1.70a	44.46 ± 1.56a	31.89 ± 2.01b
TUDCA	P-BA	T-BA	0.42 ± 0.06d	1.03 ± 0.07cd	0.75 ± 0.06d	0.87 ± 0.11d	0.88 ± 0.14d	1.54 ± 0.16bc	2.00 ± 0.27b	3.22 ± 0.10a	3.56 ± 0.18a
T(α+β)	P-BA	T-BA	7.58 ± 0.68d	11.57 ± 0.83d	7.34 ± 0.66d	16.94 ± 1.33c	18.92 ± 0.56bc	21.58 ± 1.35bc	23.91 ± 1.14b	36.29 ± 1.17a	17.77 ± 1.18c
GCDCA	P-BA	G-BA	ND	ND	ND	ND	ND	ND	ND	ND	ND
GCA	P-BA	G-BA	0.03 ± 0.01cd	0.10 ± 0.01a	0.01 ± 0.00d	0.01 ± 0.00d	0.07 ± 0.01	0.02 ± 0.01cd	0.04 ± 0.01bcd	0.06 ± 0.01bc	0.05 ± 0.01bcd
GDCA	S-BA	G-BA	ND	ND	ND	ND	ND	ND	ND	ND	ND
GUDCA	S-BA	G-BA	ND	ND	ND	ND	ND	ND	ND	ND	ND
TLCA	S-BA	T-BA	0.01 ± 0.01a	0.03 ± 0.01a	0.00 ± 0.00a	0.01 ± 0.00a	0.01 ± 0.01a	0.01 ± 0.00a	0.02 ± 0.00a	0.02 ± 0.00a	0.02 ± 0.00a
TDCA	S-BA	T-BA	1.32 ± 0.10cd	1.66 ± 0.99c	0.89 ± 0.06d	1.07 ± 0.08cd	1.42 ± 0.16cd	2.98 ± 0.11 ab	3.09 ± 0.11	2.60 ± 0.13b	3.37 ± 0.21a
THDCA	S-BA	T-BA	0.28 ± 0.02d	1.00 ± 0.09cd	0.51 ± 0.14d	0.66 ± 0.08d	0.89 ± 0.07d	0.96 ± 0.12cd	1.63 ± 0.21bc	2.71 ± 0.11a	1.99 ± 0.25b
LCA	S-BA	U-BA	ND	ND	ND	ND	ND	ND	ND	ND	ND
HDCA	S-BA	U-BA	0.00 ± 0.00a	0.00 ± 0.00a	0.00 ± 0.00a	0.00 ± 0.00a	0.00 ± 0.00a	0.01 ± 0.00a	0.01 ± 0.00a	0.00 ± 0.00a	0.00 ± 0.00a
DCA	S-BA	U-BA	ND	ND	ND	ND	ND	ND	ND	ND	ND
UDCA	S-BA	U-BA	0.02 ± 0.00c	0.05 ± 0.00b	0.02 ± 0.00c	0.01 ± 0.00c	0.05 ± 0.01b	0.03 ± 0.00bc	0.05 ± 0.01b	0.09 ± 0.01a	0.02 ± 0.01bc
Total P-BA			28.64 ± 0.61g	45.77 ± 2.20ef	37.08 ± 1.47 fg	50.77 ± 2.91de	62.16 ± 2.84cd	68.35 ± 3.23c	84.54 ± 3.44b	99.83 ± 3.71a	63.22 ± 2.92c
Total S-BA			1.64 ± 0.10cd	2.74 ± 0.17c	1.42 ± 0.14d	1.74 ± 0.16cd	2.38 ± 0.23cd	3.98 ± 0.02b	4.79 ± 0.23	5.43 ± 0.03a	5.40 ± 0.44a
Total U-BA			4.45 ± 0.19cd	8.70 ± 0.15de	8.64 ± 0.18e	7.97 ± 0.07de	12.09 ± 0.05c	12.29 ± 0.17b	14.15 ± 0.20a	15.90 ± 0.29a	9.97 ± 0.24c
Total C-BA			25.83 ± 0.41g	39.81 ± 2.41ef	29.86 ± 1.52 fg	44.53 ± 3.05de	52.45 ± 3.07cd	60.04 ± 3.39c	75.18 ± 3.73b	89.36 ± 3.46a	58.65 ± 3.15c
Total BA			30.28 ± 0.56g	48.51 ± 2.32ef	38.50 ± 1.49 fg	52.51 ± 3.00de	64.53 ± 3.04cd	72.33 ± 3.22c	89.33 ± 3.65b	105.26 ± 3.74a	68.63 ± 3.35c

Note: All data in the table are shown as mean ± SEM (n = 8). Means with different letters in the same row are significantly different using one-way ANOVA followed by the Duncan's test, *P* < 0.05.

and it potentially contributed to the regulation of cholesterol metabolism and metabolic disorders.

In addition, a large amount of CDCA was excreted in feces, especially in HFD + BM (108.15 ± 5.16 ng/mg) and HFD + BH groups (103.17 ± 5.08 ng/mg). CDCA was the main product of the alternative pathway of hepatic cholesterol metabolism, and the ingestion of BLR extract promoted the degradation of cholesterol in the liver to CDCA through the alternative pathway. The excreted CDCA facilitated the production of CDCA in the liver by negative feedback regulation. It was speculated that oxidative products in BLR extract, such as theaflavin, had positive regulatory effects on the alternative pathway of cholesterol metabolism in the liver.

3.7. The key gene expressions related to cholesterol metabolism in the liver

The treatments of LR extract and BLR extract effectively reversed the repression of cholesterol metabolism-related gene expression such as CYP7B1, CYP27A1, and FXR in the alternative pathway induced by HFD (Fig. 4 C, D, E). In particular, BLR extract consumption increased the gene expression of CYP7B1 and FXR more significantly than LR extract treatment at the same dose (*P* < 0.05). However, neither LR nor BLR extract consumption significantly altered the expression of CYP7A1 and

CYP8B1 genes in the classical pathway of cholesterol metabolism (Fig. 4 A, B, *P* > 0.05). This is in line with similar results observed in the effects of green tea phenolics and their oxidation products in obese mice, as reported by Liu et al. (2022c). Our study also provided evidence that LR extract and BLR extract had the potential to modulate cholesterol metabolism through the regulation of key genes, particularly in the alternative pathways. Moreover, it was speculated that oxidative products in BLR extract had more positive regulatory effects on the key genes of alternative pathways of cholesterol metabolism compared to bioactive compounds in LR extract.

3.8. The contents of enzymes related to ileal BAs reabsorption

LR extract or BLR extract treatment significantly reduced the content of ASBT in ileum compared with HFD group (Fig. 5 A, *P* < 0.05). The consumption of LR extract or BLR extract effectively regulated the IBABP contents to a normal level (Fig. 5 B, *P* < 0.05). The FXR contents in ileal affected by LR extract or BLR extract all decreased significantly compared with the HFD group (Fig. 5 C, *P* < 0.05). Notably, consuming BLR extract at high dose decreased the FXR content in the ileum remarkably compared with that of LR extract (*P* < 0.05). Inhibiting the transport of BAs by FXR, ASBT and IBABP is a major way to reduce intestinal BAs reabsorption (Miyata et al., 2013). Takashima et al. (2021)

Table 5
Contents of fecal bile acids after LR extract and BLR extract consumption (ng/mg).

Feces			ND	HFD	HFD+LL	HFD+LM	HFD+LH	HFD+BL	HFD+BM	HFD+BH	HFD+XZK
BA	Source	Structure									
α-MCA	P-BA	U-BA	5.39 ± 0.80e	23.11 ± 1.27cd	16.02 ± 1.52d	18.77 ± 0.51cd	23.69 ± 1.66cd	24.11 ± 1.96cd	41.04 ± 3.06a	34.04 ± 1.74 ab	26.55 ± 1.48bc
			0.05 ± 0.01e	14.65 ± 0.66cd	12.84 ± 0.46d	13.19 ± 0.68d	18.78 ± 1.32bc	19.70 ± 1.33 ab	23.57 ± 0.43a	17.98 ± 0.97bc	16.54 ± 0.86bcd
β-MCA	P-BA	U-BA	0.06 ± 0.02g	33.64 ± 1.35cd	25.89 ± 0.82ef	31.64 ± 0.79cde	35.83 ± 2.12c	26.58 ± 1.03def	42.94 ± 1.55b	57.28 ± 1.50a	23.40 ± 1.72f
			0.92 ± 0.18d	57.55 ± 1.67c	55.93 ± 2.58c	66.07 ± 1.54c	87.49 ± 2.28b	62.76 ± 2.13cd	108.15 ± 5.16a	103.17 ± 5.08a	64.90 ± 2.76c
CA	P-BA	U-BA	ND	ND	ND	ND	ND	ND	ND	ND	ND
			0.14 ± 0.04c	1.31 ± 0.12b	0.85 ± 0.07b	1.32 ± 0.09b	2.30 ± 0.11a	1.97 ± 0.09a	2.46 ± 0.12a	2.04 ± 0.15a	1.16 ± 0.08b
CDCA	P-BA	U-BA	0.00 ± 0.00c	0.10 ± 0.01b	0.03 ± 0.01cd	0.07 ± 0.01bc	0.04 ± 0.01cd	0.03 ± 0.00cd	0.21 ± 0.01a	0.24 ± 0.02a	0.06 ± 0.01bcd
			0.00 ± 0.00c	0.01 ± 0.01a	0.00 ± 0.00c	0.01 ± 0.01bc	0.00 ± 0.00c	0.01 ± 0.01bc	0.02 ± 0.00bc	0.18 ± 0.01b	0.22 ± 0.02b
DHCA	P-BA	U-BA	ND	ND	ND	ND	ND	ND	ND	ND	ND
			0.06 ± 0.01b	1.76 ± 0.14a	0.12 ± 0.03b	0.15 ± 0.04b	0.05 ± 0.01b	0.25 ± 0.02b	0.18 ± 0.02b	0.22 ± 0.04b	0.06 ± 0.01b
TCA	P-BA	T-BA	ND	ND	ND	ND	ND	ND	ND	ND	ND
			0.00 ± 0.00c	0.01 ± 0.00c	0.00 ± 0.00c	0.00 ± 0.00c	0.00 ± 0.00c	0.00 ± 0.00c	0.08 ± 0.01a	0.04 ± 0.01b	0.00 ± 0.00c
TUDCA	P-BA	T-BA	0.00 ± 0.00c	0.07 ± 0.01a	0.00 ± 0.00c	0.01 ± 0.01bc	0.00 ± 0.00c	0.01 ± 0.01bc	0.02 ± 0.00bc	0.03 ± 0.01b	0.00 ± 0.00bc
			0.00 ± 0.00c	0.01 ± 0.01a	0.00 ± 0.00c	0.01 ± 0.01bc	0.00 ± 0.00c	0.01 ± 0.01bc	0.01 ± 0.00bc	0.02 ± 0.01b	0.01 ± 0.00bc
T(α+β) MCA	P-BA	T-BA	ND	ND	ND	ND	ND	ND	ND	ND	ND
			0.00 ± 0.00e	0.15 ± 0.01d	0.16 ± 0.02cd	0.14 ± 0.02d	0.04 ± 0.02d	0.17 ± 0.03bcd	0.26 ± 0.01a	0.24 ± 0.01abc	0.24 ± 0.01ab
GCDCA	P-BA	G-BA	0.28 ± 0.04d	1.08 ± 0.06bc	1.06 ± 0.05bc	0.79 ± 0.07de	0.69 ± 0.04b	1.21 ± 0.04b	1.23 ± 0.10b	2.38 ± 0.08a	1.43 ± 0.013b
			0.00 ± 0.00d	0.12 ± 0.01cd	0.00 ± 0.00d	0.14 ± 0.01cd	0.04 ± 0.01c	0.34 ± 0.03b	0.58 ± 0.04a	0.45 ± 0.04b	0.05 ± 0.01cd
GCA	P-BA	G-BA	0.00 ± 0.00f	0.30 ± 0.03cd	0.16 ± 0.02e	0.19 ± 0.01de	0.45 ± 0.02bc	0.39 ± 0.02bc	0.22 ± 0.02de	0.55 ± 0.04a	0.28 ± 0.02d
			0.18 ± 0.04c	18.14 ± 0.86a	12.78 ± 0.68 ab	10.66 ± 2.40b	13.85 ± 0.33 ab	11.06 ± 2.04 ab	12.77 ± 1.02 ab	14.06 ± 1.18 ab	15.68 ± 0.39 ab
GDCA	S-BA	G-BA	0.00 ± 0.00d	0.57 ± 0.07bc	0.62 ± 0.09bc	0.55 ± 0.10abc	0.69 ± 0.04bc	0.66 ± 0.03a	1.01 ± 0.03a	0.91 ± 0.03bc	0.57 ± 0.05bc
			0.00 ± 0.00d	0.07 ± 0.01a	0.00 ± 0.00c	0.01 ± 0.01bc	0.00 ± 0.00c	0.01 ± 0.01bc	0.02 ± 0.01b	0.03 ± 0.01b	0.00 ± 0.00bc
GUDCA	S-BA	G-BA	ND	ND	ND	ND	ND	ND	ND	ND	ND
			0.00 ± 0.00e	0.15 ± 0.01d	0.16 ± 0.02cd	0.14 ± 0.02d	0.04 ± 0.02d	0.17 ± 0.03bcd	0.26 ± 0.01a	0.24 ± 0.01abc	0.24 ± 0.01ab
TLCA	S-BA	T-BA	0.00 ± 0.00d	0.12 ± 0.01cd	0.00 ± 0.00d	0.14 ± 0.01cd	0.04 ± 0.01c	0.34 ± 0.03b	0.58 ± 0.04a	0.45 ± 0.04b	0.05 ± 0.01cd
			0.00 ± 0.00f	0.30 ± 0.03cd	0.16 ± 0.02e	0.19 ± 0.01de	0.45 ± 0.02bc	0.39 ± 0.02bc	0.22 ± 0.02de	0.55 ± 0.04a	0.28 ± 0.02d
TDCA	S-BA	T-BA	0.18 ± 0.04c	18.14 ± 0.86a	12.78 ± 0.68 ab	10.66 ± 2.40b	13.85 ± 0.33 ab	11.06 ± 2.04 ab	12.77 ± 1.02 ab	14.06 ± 1.18 ab	15.68 ± 0.39 ab
			0.00 ± 0.00d	0.57 ± 0.07bc	0.62 ± 0.09bc	0.55 ± 0.10abc	0.69 ± 0.04bc	0.66 ± 0.03a	1.01 ± 0.03a	0.91 ± 0.03bc	0.57 ± 0.05bc
THDCA	S-BA	T-BA	ND	ND	ND	ND	ND	ND	ND	ND	ND
			6.62 ± 0.78e	132.13 ± 1.49c	111.68 ± 3.25d	131.20 ± 1.08c	168.18 ± 4.60b	135.41 ± 2.04c	218.66 ± 3.69a	215.37 ± 2.51a	132.68 ± 3.01c
LCA	S-BA	U-BA	0.46 ± 0.04c	20.43 ± 0.77a	14.77 ± 0.85 ab	12.48 ± 2.41b	15.97 ± 0.47 ab	13.83 ± 2.06 ab	16.12 ± 1.04 ab	18.62 ± 1.30 ab	18.25 ± 0.52 ab
			6.60 ± 0.79e	147.96 ± 0.88c	124.24 ± 3.95c	141.06 ± 3.36d	180.78 ± 4.20b	145.27 ± 3.06c	229.70 ± 4.04a	228.35 ± 3.81a	147.92 ± 2.74c
HDCA	S-BA	U-BA	0.48 ± 0.04h	4.59 ± 0.10bc	2.21 ± 0.15g	2.62 ± 0.14fg	3.37 ± 0.08de	3.98 ± 0.20cd	5.08 ± 0.18ab	5.64 ± 0.10a	3.00 ± 0.13ef
			7.08 ± 0.79a	152.56 ± 0.95c	126.45 ± 3.97d	143.68 ± 3.48c	184.15 ± 4.18b	149.24 ± 2.90c	234.78 ± 4.21a	233.99 ± 3.72a	150.92 ± 2.61c
DCA	S-BA	U-BA	0.00 ± 0.00d	0.57 ± 0.07bc	0.62 ± 0.09bc	0.55 ± 0.10abc	0.69 ± 0.04bc	0.66 ± 0.03a	1.01 ± 0.03a	0.91 ± 0.03bc	0.57 ± 0.05bc
			0.00 ± 0.00d	0.07 ± 0.01a	0.00 ± 0.00c	0.01 ± 0.01bc	0.00 ± 0.00c	0.01 ± 0.01bc	0.02 ± 0.01b	0.03 ± 0.01b	0.00 ± 0.00bc
UDCA	S-BA	U-BA	ND	ND	ND	ND	ND	ND	ND	ND	ND
			0.00 ± 0.00d	0.07 ± 0.01a	0.00 ± 0.00c	0.01 ± 0.01bc	0.00 ± 0.00c	0.01 ± 0.01bc	0.02 ± 0.01b	0.03 ± 0.01b	0.00 ± 0.00bc
Total P-BA			6.62 ± 0.78e	132.13 ± 1.49c	111.68 ± 3.25d	131.20 ± 1.08c	168.18 ± 4.60b	135.41 ± 2.04c	218.66 ± 3.69a	215.37 ± 2.51a	132.68 ± 3.01c
			0.46 ± 0.04c	20.43 ± 0.77a	14.77 ± 0.85 ab	12.48 ± 2.41b	15.97 ± 0.47 ab	13.83 ± 2.06 ab	16.12 ± 1.04 ab	18.62 ± 1.30 ab	18.25 ± 0.52 ab
Total S-BA			6.60 ± 0.79e	147.96 ± 0.88c	124.24 ± 3.95c	141.06 ± 3.36d	180.78 ± 4.20b	145.27 ± 3.06c	229.70 ± 4.04a	228.35 ± 3.81a	147.92 ± 2.74c
			0.48 ± 0.04h	4.59 ± 0.10bc	2.21 ± 0.15g	2.62 ± 0.14fg	3.37 ± 0.08de	3.98 ± 0.20cd	5.08 ± 0.18ab	5.64 ± 0.10a	3.00 ± 0.13ef
Total U-BA			7.08 ± 0.79a	152.56 ± 0.95c	126.45 ± 3.97d	143.68 ± 3.48c	184.15 ± 4.18b	149.24 ± 2.90c	234.78 ± 4.21a	233.99 ± 3.72a	150.92 ± 2.61c
			0.00 ± 0.00d	0.07 ± 0.01a	0.00 ± 0.00c	0.01 ± 0.01bc	0.00 ± 0.00c	0.01 ± 0.01bc	0.02 ± 0.01b	0.03 ± 0.01b	0.00 ± 0.00bc
Total C-BA			0.48 ± 0.04h	4.59 ± 0.10bc	2.21 ± 0.15g	2.62 ± 0.14fg	3.37 ± 0.08de	3.98 ± 0.20cd	5.08 ± 0.18ab	5.64 ± 0.10a	3.00 ± 0.13ef
			7.08 ± 0.79a	152.56 ± 0.95c	126.45 ± 3.97d	143.68 ± 3.48c	184.15 ± 4.18b	149.24 ± 2.90c	234.78 ± 4.21a	233.99 ± 3.72a	150.92 ± 2.61c
Total BA			6.62 ± 0.78e	132.13 ± 1.49c	111.68 ± 3.25d	131.20 ± 1.08c	168.18 ± 4.60b	135.41 ± 2.04c	218.66 ± 3.69a	215.37 ± 2.51a	132.68 ± 3.01c
			0.46 ± 0.04c	20.43 ± 0.77a	14.77 ± 0.85 ab	12.48 ± 2.41b	15.97 ± 0.47 ab	13.83 ± 2.06 ab	16.12 ± 1.04 ab	18.62 ± 1.30 ab	18.25 ± 0.52 ab

Note: All data in the table are shown as mean ± SEM (n = 8). Means with different letters in the same row are significantly different using one-way ANOVA followed by the Duncan's test, $P < 0.05$.

found theaflavin had a modulatory effect on ASBT, suggesting that theaflavin in BLR extract may play a pivotal role in inhibiting BAS reabsorption. This mechanism aligns with our observations of reduced ASBT levels in the ileum after consuming LR extract and BLR extract. These findings underscored the potential significance of theaflavin in BLR extract and its impact on BAS dynamics in the enterohepatic circulation. Also, the intricate interplay between specific compounds in BLR extract and BAS reabsorption mechanisms warranted further exploration. It could provide valuable insights into its therapeutic applications in managing cholesterol metabolism and related health conditions.

3.9. The key gene and protein expression levels of FXR and FGF15 in the ileum

Compared with the ND group, HFD dramatically induced the increase of FXR and FGF15 gene expression ($P < 0.05$, Fig. 6A and B). A significant decrease in ileal FXR mRNA transcription was detected in the HFD + LH, HFD + BM, and HFD + BH groups compared to the HFD group ($P < 0.05$). The consumption of BLR extract at medium or high doses dramatically inhibited the increase of the mRNA expression of

ileal FGF15 induced by HFD ($P < 0.05$). However, the consumption of LR extract did not show the inhibition effects on the mRNA expression of ileal FGF15 ($P > 0.05$).

The consumption of BLR extract had more pronounced down-regulation effect on FXR and FGF15 relative protein expression compared to that of LR extract (Fig. 6, C, D, and E). BLR extract treatment on the HFD mice significantly downregulated the protein expression of FXR compared to LR treatment at the same doses ($P < 0.05$). However, only the intakes of LR extract at medium and high doses significantly reduced the rise of FXR induced by HFD. The consumption of BLR extract at a medium dose was more effective than that of LR extract in reducing the ileal proteins expression of FGF15 ($P < 0.05$). These findings suggested that BLR extract may inhibit the upregulation expression of FXR and FGF15 proteins in the ileum effectively. The suppression of the ileal FXR-FGF15 signaling pathway has been linked to elevated hepatic BAS production and reduced cholesterol deposition in the liver, offering potential benefits for NAFLD (Degirolamo et al., 2014; Li et al., 2013). Similarly, recent research demonstrated that the cholesterol-lowering effects of theabrownin are attributed to the inhibition of the ileal FXR-FGF15 signaling pathway, suggesting it was a promising way for anti-hypercholesterolemia (Huang et al., 2019). Our

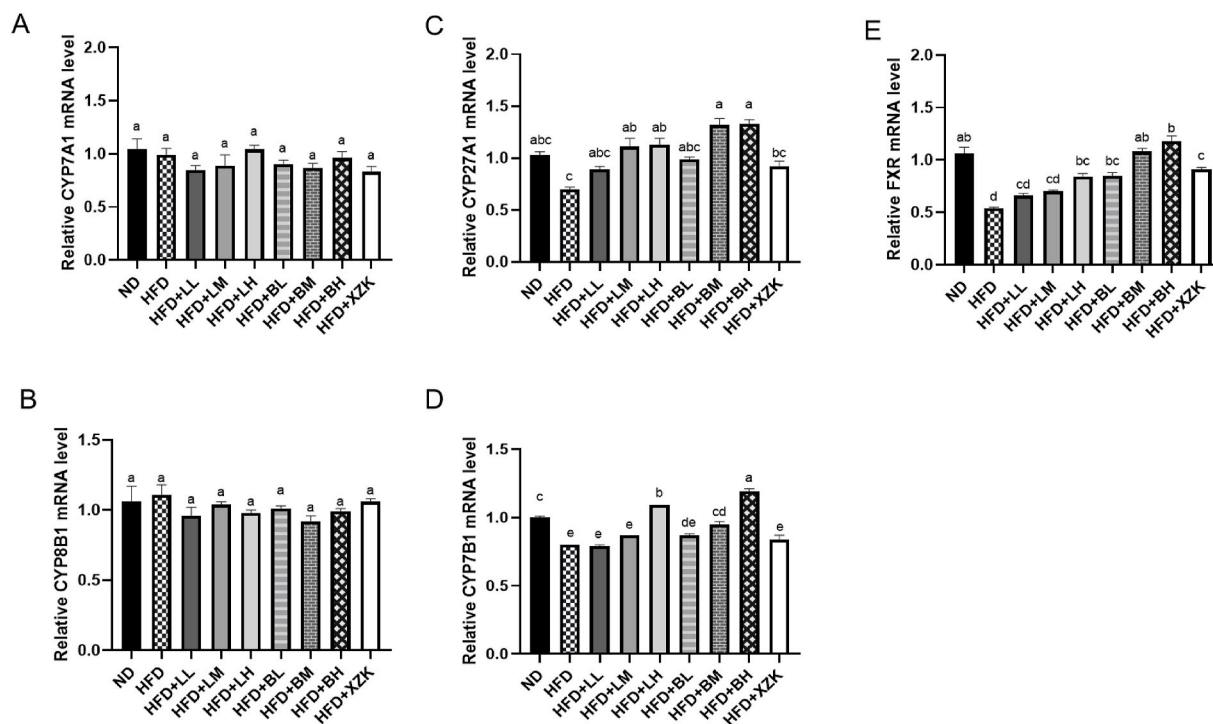


Fig. 4. Effects of LR extract and BLR extract on mRNA expression related to cholesterol metabolism in the liver. (A) Relative CYP7A1 mRNA level; (B) Relative CYP8B1 mRNA level; (C) Relative CYP27A1 mRNA level; (D) Relative CYP7B1 mRNA level; (E) Relative FXR mRNA level. Bars with various letters differ significantly using one-way ANOVA followed by the Duncan's test, $P < 0.05$.

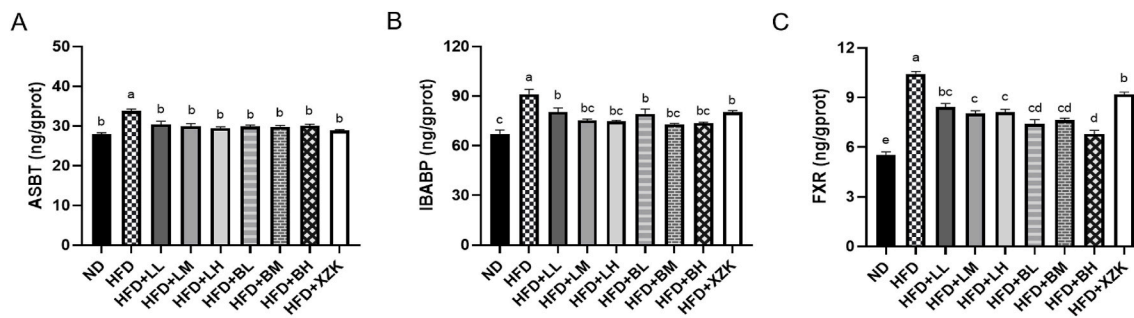


Fig. 5. Effects of LR extract and BLR extract on the contents of factors related to bile acids (BAs) reabsorption in the ileum. (A) The contents of apical sodium-dependent bile acid transporter (ASBT); (B) The contents of ileal bile acid binding protein (IBABP); (C) The contents of FXR. Bars with various letters differ significantly using one-way ANOVA followed by the Duncan's test, $P < 0.05$.

study results further emphasized the potential of BLR extract in modulating the ileal FXR-FGF15 signaling pathway, which may contribute to its cholesterol-lowering effects and pivotal role in managing conditions like NAFLD and hypercholesterolemia.

3.10. Effects of LR extract and BLR extract on gut microbiota

The impacts of administering LR extract and BLR extract on the gut microbiota are shown in Fig. 7. The consumption of LR extract and BLR extract at low, medium, and high doses led to notable variations in the gut microbiota profile, as indicated by PCoA analysis (Fig. 7 A, B, C). At the phylum level, *Bacteroides* and *Firmicutes* were found to be the predominant phyla among 10 phyla across all groups (Fig. 7 D). HFD significantly elevated the *Firmicutes/Bacteroidetes* ratios compared to the ND group (Fig. 7 E, $P < 0.05$). The administrations of LR extract and BLR extract exhibited significant effects on reducing the ratios of *Firmicutes/Bacteroidetes*. The high dose of BLR extract demonstrated the most pronounced effect on *Firmicutes/Bacteroidetes* ratio reduction.

The heatmap analysis is based on the species composition and

relative abundance of each sample group, using color gradients to depict the similarities and differences in the community compositions among different groups. As shown in Fig. 7 F, the abundance of *Bacteroides*, *Blautia*, and *Ruminiclostridium_6* was relatively high in the ND group. However, a significant increase in the abundance of *Desulfovibrio* and *unclassified_Erysipelotrichaceae* was observed in the gut of HFD-fed mice. The rise of *Desulfovibrio* was observed in the intestine of humans with obesity and type 2 diabetes, suggesting that the increase of *Desulfovibrio* might be relevant to metabolic disease (Wang and Hooper, 2019). Both LR extract and BLR extract exhibited a remarkable reduction in *Desulfovibrio* abundance, even at low dose (Fig. 7 G). Moreover, for LR extract, the low-dose group exhibited an elevation in the abundance of *Lachnospiraceae_NK4A136_group*. The medium-dose LR extract significantly increased the abundance of *Ruminococcaceae_UCG-014*, *uncultured_bacterium_o_Mollicutes_RF39*, and *Prevotellaceae_UCG-001*. In the high dose group, there was a substantial increase in the abundance of *Lactobacillus* and *Candidatus_Pelagibacter*. It's worth highlighting that the abundance of *Lactobacillus* significantly increased under the LR extract treatment at low, medium, and high doses, while there was no significant increase

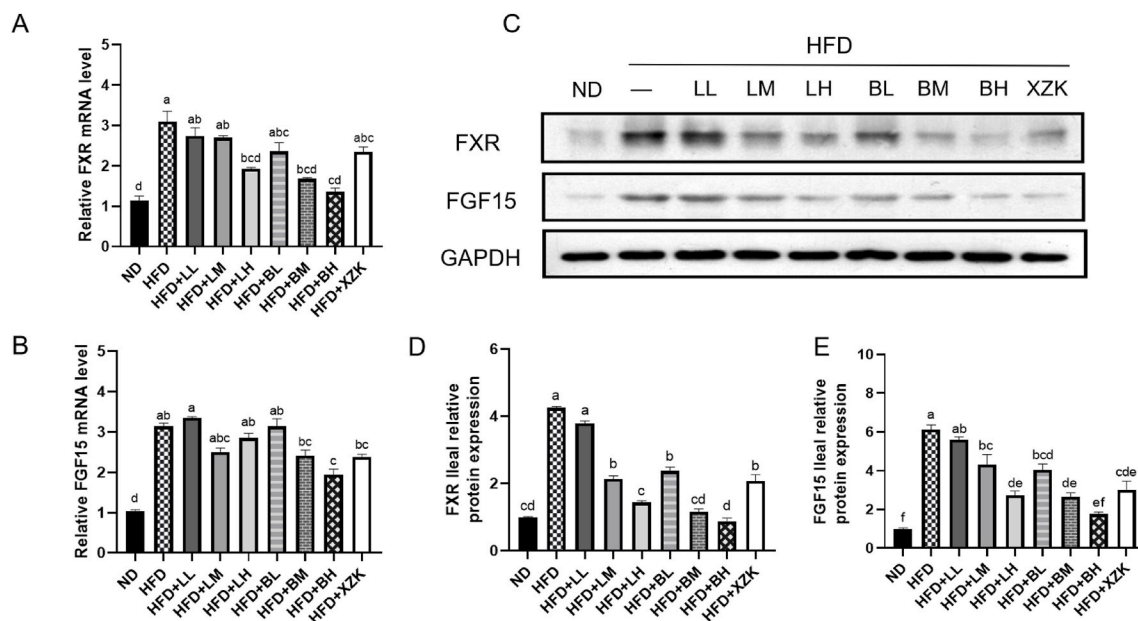


Fig. 6. Effects of LR extract and BLR extract on gene expression and protein expression levels of FXR and FGF15 in ileum. (A) Relative farnesoid x receptor (FXR) mRNA levels; (B) Relative fibroblast growth factor 15 (FGF15) mRNA levels; (C) The protein expression of FXR and FGF15 measured by western blot analysis; (D) FXR relative protein expression levels; (E) FGF15 relative protein expression levels. Bars with various letters differ significantly using one-way ANOVA followed by the Duncan's test, $P < 0.05$.

observed in BLR groups (Fig. 7 H). Previous research confirmed that *Lactobacillus* is beneficial for BAs metabolism, and *Lactobacillus* can modulate BAs enterohepatic circulation (Prete et al., 2020; Zhai et al., 2019). It is speculated that LR extract primarily modulated BAs metabolism by increasing the abundance of *Lactobacillus* in the gut. This elevation in *Lactobacillus* abundance, especially in response to high dose of LR extract, suggests that *Lactobacillus* plays a crucial role in regulating BAs homeostasis.

For BLR extract treatment, the low-dose group exhibited an increased abundance of *Alloprevotella*. In the medium-dose group, there was a slight rise in the abundance of *Lachnospiraceae NK4A136 group* and *Prevotellaceae UCG-001*. In the high-dose group, the most notable increase was observed in the abundance of *Akkermansia* and *Lachnoclostridium*. Importantly, the increase in *Akkermansia* abundance displayed a dose-dependent relationship with the BLR extract, with higher dose resulting in more significant increase (Fig. 7 I). Previous studies have highlighted the role of *Akkermansia* in regulating the intestinal FXR-FGF15 axis and reshaping BAs profiles, underlining its potential significance in managing metabolic-associated fatty liver disease (MAFLD) (Wu et al., 2023). These findings aligned with our current study and suggested that the modulation of *Akkermansia* abundance by BLR extract might be a pivotal factor contributing to regulating cholesterol metabolism disorders. Our results provide valuable insights into the potential mechanisms underlying the cholesterol-lowering effects of LR extract and BLR extract, with *Lactobacillus* enrichment linked to LR extract and *Akkermansia* abundance associated with BLR extract. These observations strengthen the foundation for exploring these natural extracts as potential therapies for hypercholesterolemia and metabolic disorders.

LR is prone to oxidize and brown during storage or after being mechanically damaged. However, the result showed that in the BLR extract, there were still some bioactive components remained or formed, and the main oxidation product of catechins catalyzed by PPO was theaflavin. As shown in Fig. 8, the consumption of LR extract or BLR extract increased the synthesis of BAs in liver, which indicated that more cholesterol was metabolized into BAs. Meanwhile, the intake of LR extract or BLR extract remarkably promoted the excretion of BAs in feces.

Furthermore, FXR played different roles in the liver and ileum. Promoting hepatic FXR activated the alternative pathway of cholesterol

metabolism, while inhibiting ileal FXR alleviated the inhibition of ileal FXR-FGF15 pathway on cholesterol degradation and decreased the reabsorption of BAs in the ileum. The consumption of LR extract or BLR extract activated hepatic FXR, and shifted BAs biosynthesis from the classical pathway to the alternative pathway to a certain extent. In addition, LR extract or BLR extract treatment also alleviated the inhibition of key gene and protein expressions in the FXR-FGF15 pathway. In detail, the consumption of LR extract or BLR extract inhibited the expression of ileal FXR and reduced the production of the hormone FGF15. The FGF15 circulated to the liver and then alleviated the restriction of FXR-FGF15 pathway on BAs synthesis. In addition, LR extract or BLR extract treatment also decreased the content of reabsorption-related enzymes including FXR, ABST and IBABP. Besides, the altered BAs composition especially T($\alpha+\beta$)MCA, TCA, and CDCA affected the expression of hepatic and ileal FXR genes. The increased excretion of CDCA in feces facilitated the production of CDCA in liver by negative feedback regulation. Therefore, all these changes affected by the consumption of LR extract or BLR extract regulated the disorder of cholesterol metabolism induced by HFD. Moreover, LR extract and BLR extract ameliorated the enrichment of detrimental gut bacteria, such as *Desulfovibrio*, induced by HFD, while increasing the abundance of beneficial probiotics. These probiotics like *Lactobacillus* and *Akkermansia* hold promise in ameliorating the disturbances in cholesterol metabolism caused by HFD through their role in regulating BA metabolism.

Notably, the consumption of BLR extract was more effective than that of LR extract in reducing the ileal gene and protein expressions of FXR and FGF15, activating the hepatic gene expressions of FXR and CYP7B1 in the alternative pathway. BLR promoted cholesterol metabolism to produce BAs in the liver and increased the excretion of BAs in feces, thus the intake of BLR extract showed more effective results in regulating cholesterol metabolism. Furthermore, the BLR extract exhibited the potential to effectively modulate cholesterol metabolism of HFD-fed mice by significantly increasing the abundance of the beneficial probiotic, *Akkermansia*, which was known to play a typical role in regulating the intestinal FXR-FGF15 axis and reshaping BAs profiles. Conversely, LR extract, demonstrated a pronounced enrichment of another probiotic, *Lactobacillus*. This suggested that the unique compositions of the bioactive components in LR extract and BLR extract

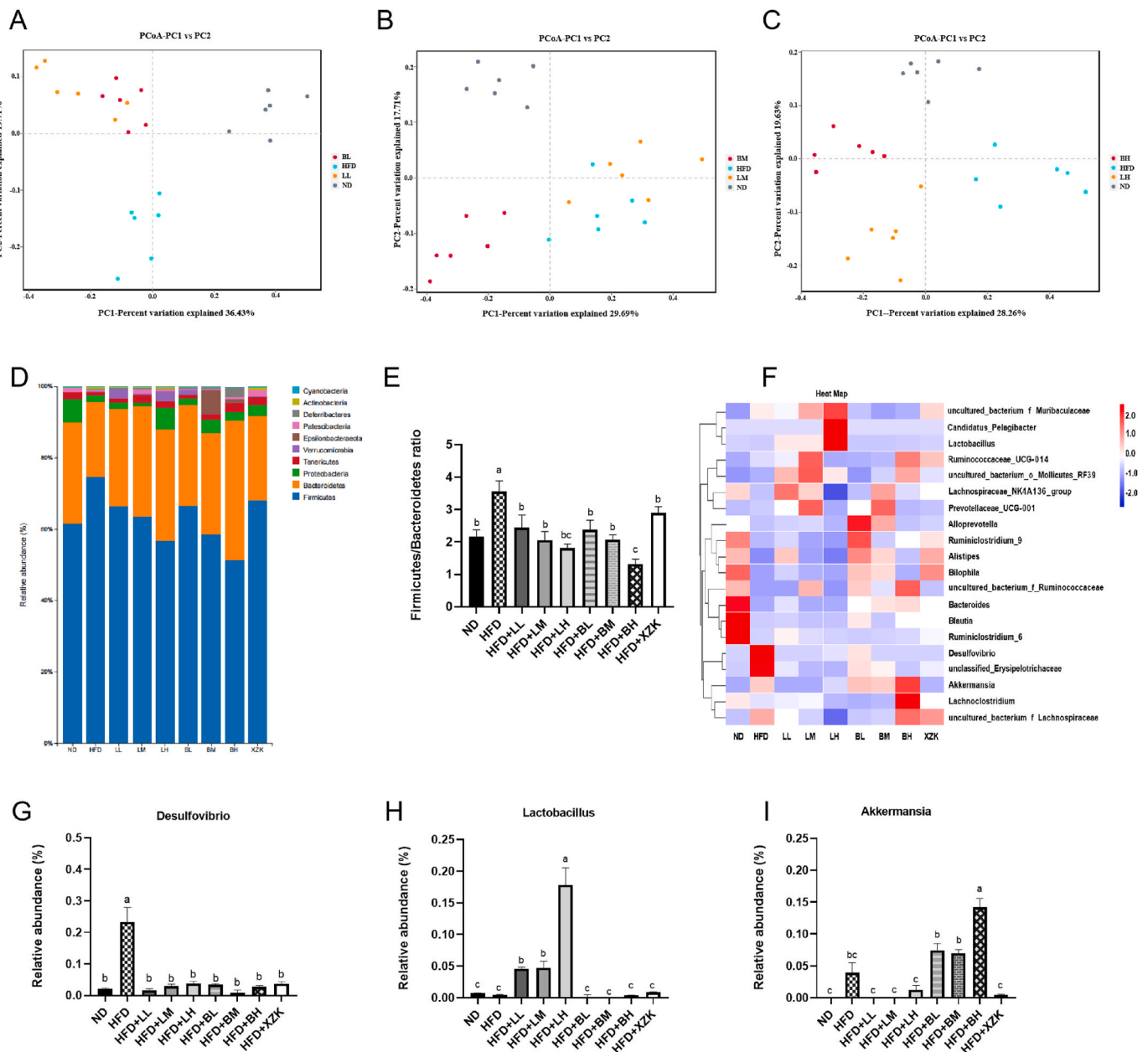


Fig. 7. Effects of LR extract and BLR extract on the composition of the gut microbiota in mice. A. β -diversity analysis was performed by principal coordinate analysis (PCoA) at low dose (100 mg/kg/d); B. β -diversity analysis was performed by PCoA at low dose (400 mg/kg/d); C. β -diversity analysis was performed by PCoA at low dose (1200 mg/kg/d); D. Relative abundance of the top 10 abundant bacteria at the phylum level; E. Ratio of *Firmicutes* to *Bacteroidetes*; F. Taxa heatmap at genus levels. G. Relative abundances of *Desulfovibrio* affected by LR extract or BLR extract; H. Relative abundances of *Lactobacillus* affected by LR extract or BLR extract; I. Relative abundances of *Akkermansia* affected by LR extract or BLR extract. Data are expressed as mean \pm SEM (n = 6). Different superscripts (a, b, c) represent significant differences from each other; $P < 0.05$.

resulted in varying impacts on gut microbiota. These differential effects lead to distinct mechanisms in cholesterol metabolism disorders. To some extent, our research revealed that BLR extract even showed more robust modulatory effects on cholesterol metabolism than LR extract. Thus, BLR and its leftovers should be more fully utilized to avoid the serious waste of lotus resources.

4. Conclusion

In this study, the content of main phenolic compound catechin decreased sharply while the theaflavin content increased dramatically in BLR, which indicated that a large amount of catechins are oxidized to theaflavin during the browning process of LR. The consumption of LR or

BLR extract promoted cholesterol to produce BAs in the liver of HFD mice and increased the BAs excreted in feces. Both LR extract and BLR extract regulated cholesterol metabolism disorder. Noteworthy, the consumption of BLR extract more effectively regulated hepatic gene expressions of FXR and CYP7B1, as well as alleviated the suppression of key mRNA and protein expressions of FXR-FGF15 signaling pathway than that of LR extract. Furthermore, the influence on the gut microbiota in HFD-fed mice differed between LR extract and BLR extract: LR extract promoted the increase in the abundance of *Lactobacillus*, while BLR extract significantly elevated the abundance of *Akkermansia*. In conclusion, both LR extract and BLR extract modulated the disorders of cholesterol metabolism induced by HFD, and BLR extract even showed more robust effects on regulating the key gene and protein expressions

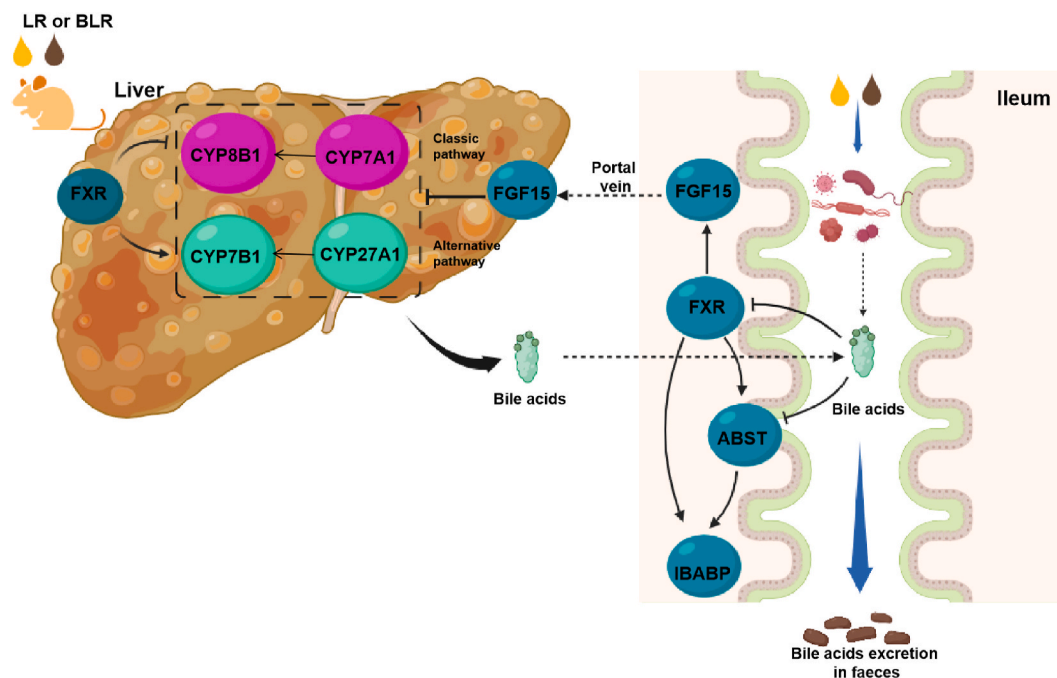


Fig. 8. Proposed cholesterol-lowering mechanism of LR extract and BLR extract.

of cholesterol metabolism.

CRediT authorship contribution statement

Jingfang Li: Conceptualization, Methodology, Formal analysis, Data curation, Writing - original draft. **Ting Luo:** Visualization, Writing - review & editing. **Xiaoping Li:** Software, Methodology. **Xiaoru Liu:** Supervision, Writing - review & editing, Funding acquisition. **Ze-yuan Deng:** Supervision, Writing - review & editing, Funding acquisition.

Declaration of competing interest

The authors declare that they have no known competing financial interests or personal relationships that could have appeared to influence the work reported in this paper.

Data availability

Data will be made available on request.

Acknowledgments

This work was financially supported by the Central Government Guide Local Special Fund Project for Scientific and Technological Development of Jiangxi Province (20221ZDD02001); Goal oriented project of State Key Laboratory of Food Science and Technology (SKLF-ZZA-202210). National Natural Science Foundation of China (No. 32260565 & 31860430). Thanks to Prof. Guodong Zhang (The National University of Singapore) for his support and assistance to Jingfang Li during her visiting study at the National University of Singapore.

Appendix A. Supplementary data

Supplementary data to this article can be found online at <https://doi.org/10.1016/j.crfs.2023.100630>.

References

- Cao, J., Yu, X., Deng, Z., Pan, Y., Zhang, B., Tsao, R., Li, H., 2018. Chemical compositions, antiobesity, and antioxidant effects of proanthocyanidins from Lotus seed epicarp and Lotus seed pot. *J. Agric. Food Chem.* 66 (51), 13492–13502.
- Chen, S., Wang, R., Cheng, M., Wei, G., Du, Y., Fan, Y., Li, J., Li, H., Deng, Z., 2020. Serum cholesterol-lowering activity of β -sitosterol laurate is attributed to the reduction of both cholesterol absorption and bile acids reabsorption in hamsters. *J. Agric. Food Chem.* 68 (37), 10003–10014.
- Cheng, H., Xu, N., Zhao, W., Su, J., Liang, M., Xie, Z., et al., 2017. (-)-Epicatechin regulates blood lipids and attenuates hepatic steatosis in rats fed high-fat diet. *Mol. Nutr. Food Res.* 61 (11), 1700303.
- Clifford, B.L., Sedgeman, L.R., Williams, K.J., Morand, P., Cheng, A., Jarrett, K.E., et al., 2021. FXR activation protects against NAFLD via bile-acid-dependent reductions in lipid absorption. *Cell Metabol.* 33 (8), 1671–1684.
- Dawson, P.A., 2018. Bile formation and the enterohepatic circulation. *Physiology of the gastrointest. tract* 931–956.
- Degirolamo, C., Rainaldi, S., Bovenga, F., Murzilli, S., Moschetta, A., 2014. Microbiota modification with probiotics induces hepatic bile acid synthesis via downregulation of the Fxr-Fgf15 axis in mice. *Cell Rep.* 7 (1), 12–18.
- Du, Y., Chen, S., Zhu, H., Niu, X., Li, J., Fan, Y., Deng, Z., 2020. Consumption of interesterified medium-and long-chain triacylglycerols improves lipid metabolism and reduces inflammation in high-fat diet-induced obese rats. *J. Agric. Food Chem.* 68 (31), 8255–8262.
- Fraser, K., Lane, G.A., Otter, D.E., Harrison, S.J., Quek, S.Y., Hemar, Y., Rasmussen, S., 2014. Non-targeted analysis by LC-MS of major metabolite changes during the oolong tea manufacturing in New Zealand. *Food Chem.* 151, 394–403.
- Guo, S., Peng, Y., Lou, Y., Cao, L., Liu, J., Lin, N., Cai, S., Kang, Y., Zeng, S., Yu, L., 2022. Downregulation of the farnesoid X receptor promotes colorectal tumorigenesis by facilitating enterotoxigenic *Bacteroides fragilis* colonization. *Pharmacol. Res.* 177, 106101.
- Huang, F., Zheng, X., Ma, X., Jiang, R., Zhou, W., Zhou, S., et al., 2019. Theabrownin from Pu-erh tea attenuates hypercholesterolemia via modulation of gut microbiota and bile acid metabolism. *Nat. Commun.* 10 (1), 1–17.
- Iamtham, S., Kaewkam, A., Chanprame, S., Pan-utai, W., 2022. Effect of *Spirulina biomass* residue on yield and cordycepin and adenosine production of *Cordyceps militaris* culture. *Bioresour. Technol. Rep.* 17, 100893.
- Ikeda, I., Yamahira, T., Kato, M., Ishikawa, A., 2010. Black-tea polyphenols decrease micellar solubility of cholesterol in vitro and intestinal absorption of cholesterol in rats. *J. Agric. Food Chem.* 58 (15), 8591–8595.
- Jia, W., Wei, M., Rajani, C., Zheng, X., 2021. Targeting the alternative bile acid synthetic pathway for metabolic diseases. *Protein Cell* 12 (5), 411–425.
- Jiang, J., Jiang, L., Zhang, L., Luo, H., Opiyo, A.M., Yu, Z., 2012. Changes of protein profile in fresh-cut lotus tuber before and after browning. *J. Agric. Food Chem.* 60 (15), 3955–3965.
- Jin, D., Xu, Y., Mei, X., Meng, Q., Gao, Y., Li, B., Tu, Y., 2013. Antiobesity and lipid lowering effects of theaflavins on high-fat diet induced obese rats. *J. Funct. Foods* 5 (3), 1142–1150.

- La, M., Zhang, F., Gao, S., Liu, X., Wu, Z., Sun, L., Tao, X., Chen, W., 2015. Constituent analysis and quality control of *Lamiophlomis rotata* by LC-TOF/MS and HPLC-UV. *J. Pharmaceut. Biomed.* 102, 366–376.
- Li, B., Fu, L., Kojima, R., Yamamoto, A., Ueno, T., Matsui, T., 2021. Theaflavins prevent the onset of diabetes through ameliorating glucose tolerance mediated by promoted incretin secretion in spontaneous diabetic Torii rats. *J. Funct. Foods* 86, 104702.
- Li, F., Jiang, C., Krausz, K.W., Li, Y., Albert, L., Hao, H., Fabre, K.M., Mitchell, J.B., Patterson, A.D., Gonzalez, F.J., 2013. Microbiome remodelling leads to inhibition of intestinal farnesoid X receptor signalling and decreased obesity. *Nat. Commun.* 4 (1), 1–10.
- Li, J., Qin, Y., Yu, X., Xiong, Z., Zheng, L., Sun, Y., Shen, J., Guo, N., Tao, L., Deng, Z., 2019. In vitro simulated digestion and in vivo metabolism of chlorogenic acid dimer from *Gynura procumbens* (Lour.) Merr.: enhanced antioxidant activity and different metabolites of blood and urine. *J. Food Biochem.* 43 (6), e12654.
- Liao, T., Liu, J., Sun, Y., Zou, L., Zhou, L., Liu, C., Terefe, N.S., Liu, W., 2020. Differential inhibitory effects of organic acids on pear polyphenol oxidase in model systems and pear puree. *LWT—Food Sci. Technol.* 118, 108704.
- Liao, C.C., Ou, T.T., Wu, C.H., Wang, C.J., 2013. Prevention of diet-induced hyperlipidemia and obesity by caffeic acid in C57BL/6 mice through regulation of hepatic lipogenesis gene expression. *J. Agric. Food Chem.* 61 (46), 11082–11088.
- Limwachiranon, J., Huang, H., Shi, Z., Li, L., Luo, Z., 2018. Lotus flavonoids and phenolic acids: health promotion and safe consumption dosages. *Compr. Rev. Food Sci. F* 17 (2), 458–471.
- Lin, C., Huang, H., Lin, J., 2007. Theaflavins attenuate hepatic lipid accumulation through activating AMPK in human HepG2 cells. *J. Lipid Res.* 48 (11), 2334–2343.
- Ling, C., Xu, J., Li, Y., Tong, X., Yang, H., Yang, J., Yu, L., Qin, L., 2019. Lactoferrin promotes bile acid metabolism and reduces hepatic cholesterol deposition by inhibiting the farnesoid X receptor (FXR)-mediated enterohepatic axis. *Food Funct.* 10 (11), 7299–7307.
- Liu, C., Zhen, D., Du, H., Gong, G., Wu, Y., Ma, Q., Quan, Z., 2022a. Synergistic anti-inflammatory effects of peimine, peiminine, and forsythoside a combination on LPS-induced acute lung injury by inhibition of the IL-17-NF- κ B/MAPK pathway activation. *J. Ethnopharmacol.* 295, 115343.
- Liu, S., Wang, Q., Ma, J., Wang, J., Wang, H., Liu, L., et al., 2022. Dietary *Forsythia suspensa* extracts supplementation improves antioxidant status, anti-inflammatory functions, meat fatty acid deposition, and intestinal microbial community in finishing pigs. *Front. Vet. Sci.* 9, 960242.
- Liu, Y., Chen, Q., Liu, D., Yang, L., Hu, W., Kuang, L., Huang, Y., Teng, J., Liu, Y., 2022b. Multi-omics and enzyme activity analysis of flavour substances formation: major metabolic pathways alteration during Congou black tea processing. *Food Chem.* 403, 134263.
- Liu, Z., Chen, Q., Zhang, C., Ni, L., 2022c. Comparative study of the anti-obesity and gut microbiota modulation effects of green tea phenolics and their oxidation products in high-fat-induced obese mice. *Food Chem.* 367, 130735.
- Mahfuz, S., Shang, Q., Piao, X., 2021. Phenolic compounds as natural feed additives in poultry and swine diets: a review. *J. Anim. Sci. Biotechnol.* 12 (1), 48.
- Marchetti, L., Pellati, F., Graziosi, R., Brighenti, V., Pinetti, D., Bertelli, D., 2019. Identification and determination of bioactive phenylpropanoid glycosides of *Aloysia polystachya* (Griseb. et Moldenke) by HPLC-MS. *J. Pharmaceut. Biomed.* 166, 364–370.
- Mareček, V., Mikýška, A., Hampel, D., Čejka, P., Neuwirthová, J., Malachová, A., Cerkal, R., 2017. ABTS and DPPH methods as a tool for studying antioxidant capacity of spring barley and malt. *J. Cereal. Sci.* 73, 40–45.
- Min, T., Xie, J., Zheng, M., Yi, Y., Hou, W., Wang, L., Ai, Y., Wang, H., 2017. The effect of different temperatures on browning incidence and phenol compound metabolism in fresh-cut lotus (*Nelumbo nucifera* G.) root. *Postharvest Biol. Technol.* 123, 69–76.
- Miyata, M., Yamakawa, H., Hayashi, K., Kuribayashi, H., Yamazoe, Y., Yoshinari, K., 2013. Ileal apical sodium-dependent bile acid transporter protein levels are down-regulated through ubiquitin-dependent protein degradation induced by bile acids. *Eur. J. Pharmacol.* 714 (1–3), 507–514.
- Moreno-González, R., Juan, M.E., Planas, J.M., 2020. Profiling of pentacyclic triterpenes and polyphenols by LC-MS in Arbequina and Empeltre table olives. *LWT—Food Sci. Technol.* 126, 109310.
- Nair, A.B., Jacob, S., 2016. A simple practice guide for dose conversion between animals and human. *J. Basic Clin. Physiol. Pharmacol.* 7 (2), 27.
- Ojwang, L.O., Yang, L., Dykes, L., Awika, J., 2013. Proanthocyanidin profile of cowpea (*Vigna unguiculata*) reveals catechin-O-glucoside as the dominant compound. *Food Chem.* 139 (1–4), 35–43.
- Pan, H., Gao, Y., Tu, Y., 2016. Mechanisms of body weight reduction by black tea polyphenols. *Molecules* 21 (12), 1659.
- Pandak, W.M., Kakiyama, G., 2019. The acidic pathway of bile acid synthesis: not just an alternative pathway. *Liver Res.* 3 (2), 88–98.
- Park, S.Y., Bok, S.H., Jeon, S.M., Yong, B.P., Lee, S.J., Jeong, T.S., Choi, M.S., 2002. Effect of rutin and tannic acid supplements on cholesterol metabolism in rats. *Nutr. Res.* 22 (3), 283–295.
- Prete, R., Long, S.L., Gallardo, A.L., Gahan, C.G., Corsetti, A., Joyce, S.A., 2020. Beneficial bile acid metabolism from *Lactobacillus plantarum* of food origin. *Sci. Rep.-Uk* 10 (1), 1165.
- Santos, S.A., Freire, C.S., Domingues, M.R.M., Silvestre, A.J., Neto, C.P., 2011. Characterization of phenolic components in polar extracts of *Eucalyptus globulus* Labill. bark by high-performance liquid chromatography–mass spectrometry. *J. Agric. Food Chem.* 59 (17), 9386–9393.
- Sayin, S.I., Wahlström, A., Felin, J., Jäntti, S., Marschall, H., Bamberg, K., Angelin, B., Hyötyläinen, T., Orešič, M., Bäckhed, F., 2013. Gut microbiota regulates bile acid metabolism by reducing the levels of tauro-beta-muricholic acid, a naturally occurring FXR antagonist. *Cell Metabol.* 17 (2), 225–235.
- Showkat, Q.A., Rather, J.A., Jabeen, A., Dar, B.N., Makroo, H.A., et al., 2021. Bioactive components, physicochemical and starch characteristics of different parts of lotus (*Nelumbo nucifera* Gaertn.) plant: a review. *Int. J. Food Sci. Technol.* 56 (5), 2205–2214.
- Shukla, V., Singh, P., Konwar, R., Singh, B., Kumar, B., 2021. Phytochemical analysis of high value medicinal plant *Valeriana jatamansi* using LC-MS and its in-vitro anti-proliferative screening. *Phytomedicine* 1 (2), 100025.
- Stancu, C., Sima, A., 2001. Statins: mechanism of action and effects. *J. Cell Mol. Med.* 5 (4), 378–387.
- Sun, Q.R., Liu, P., Hui-Wei, L.I., Liu, L., Sai-Jia, N.I., Xue, F., Shang, E., Duan, J.A., 2018. Analysis and evaluation of main nutritional ingredients in residual of lotus root from different areas. *Sci. Technol. Food Ind.* 39 (6), 291–297.
- Sun, Y., Li, H., Hu, J., Li, J., Fan, Y., Liu, X., Deng, Z., 2013. Qualitative and quantitative analysis of phenolics in *Tetragium hemsleyanum* and their antioxidant and antiproliferative activities. *J. Agric. Food Chem.* 61 (44), 10507–10515.
- Sun, Y., Qin, Y., Li, H., Peng, H., Chen, H., Xie, H., Deng, Z., 2015. Rapid characterization of chemical constituents in *Radix Tetragium*, a functional herbal mixture, before and after metabolism and their antioxidant/antiproliferative activities. *J. Funct. Foods* 18, 300–318.
- Sun, Y., Tsao, R., Chen, F., Li, H., Wang, J., Peng, H., Zhang, K., Deng, Z., 2017. The phytochemical composition, metabolites, bioavailability and in vivo antioxidant activity of *Tetragium hemsleyanum* leaves in rats. *J. Funct. Foods* 30, 179–193.
- Takahashi, Y., Ishikawa, K., Miyawaki, R., Ogawa, M., Ishii, T., Misaka, T., Kobayashi, S., 2021. Modulatory effect of theaflavins on apical sodium-dependent bile acid transporter (ASBT) activity. *J. Agric. Food Chem.* 69 (33), 9585–9596.
- Toma, L., Sanda, G.M., Niculescu, L.S., Deleanu, M., Sima, A.V., Stancu, C.S., 2020. Phenolic compounds exerting lipid-regulatory, anti-inflammatory and epigenetic effects as complementary treatments in cardiovascular diseases. *Biomolecules* 10 (4), 641.
- Tsuruta, Y., Nagao, K., Shirouchi, B., Nomura, S., Tsuge, K., Koganemaru, K., et al., 2012. Effects of lotus root (the edible rhizome of *Nelumbo nucifera*) on the development of non-alcoholic fatty liver disease in obese diabetic db/db mice. *Biosci. Biotech. Biochem.* 76 (3), 462–466.
- Uriarte, I., Fernandez-Barrera, M.G., Monte, M.J., Latasa, M.U., Chang, H.C., Carotti, S., Vespasiani-Gentilucci, U., Morini, S., Vicente, E., Concepcion, A.R., Medina, J.F., Marin, J.G., Berasain, C., Prieto, J., Avila, M.A., 2013. Identification of fibroblast growth factor 15 as a novel mediator of liver regeneration and its application in the prevention of post-resection liver failure in mice. *Gut* 62 (6), 899–910.
- Wang, Y., Hooper, L.V., 2019. Immune control of the microbiota prevents obesity. *Science* 365 (6451), 316–317.
- Ward, N.C., Watts, G.F., Eckel, R.H., 2019. Statin toxicity: mechanistic insights and clinical implications. *Circ. Res.* 124 (2), 328–350.
- Wu, W., Kaicen, W., Bian, X., Yang, L., Ding, S., Li, Y., et al., 2023. Akkermansia muciniphila alleviates high-fat-diet-related metabolic-associated fatty liver disease by modulating gut microbiota and bile acids. *Microb. Biotechnol.* 00, 1–16.
- Ye, F., Liang, Q., Li, H., Zhao, G., 2015. Solvent effects on phenolic content, composition, and antioxidant activity of extracts from florets of sunflower (*Helianthus annuus* L.). *Ind. Crop. Prod.* 76, 574–581.
- You, J.S., Lee, Y.J., Kim, K.S., Kim, S.H., Chang, K.J., 2014. Ethanol extract of lotus (*Nelumbo nucifera*) root exhibits an anti-adipogenic effect in human pre-adipocytes and anti-obesity and anti-oxidant effects in rats fed a high-fat diet. *Nutr. Res.* 34 (3), 258–267.
- Zanotti, I., Dall'Asta, M., Mena, P., Mele, L., Bruni, R., Ray, S., Del Rio, D., 2015. Atheroprotective effects of (poly) phenols: a focus on cell cholesterol metabolism. *Food Funct.* 6 (1), 13–31.
- Zhai, Q., Liu, Y., Wang, C., Qu, D., Zhao, J., Zhang, H., Tian, F., Chen, W., 2019. *Lactobacillus plantarum* CCFM8661 modulates bile acid enterohepatic circulation and increases lead excretion in mice. *Food Funct.* 10 (3), 1455–1464.
- Zhang, G., Yang, J., Cui, D., Zhao, D., Benedito, V.A., Zhao, J., 2020. Genome-wide analysis and metabolic profiling unveil the role of peroxidase CsGPX3 in theaflavin production in black tea processing. *Food Res. Int.* 137, 109677.
- Zhang, J., Zhou, X., Wang, X., Zhang, J., Yang, M., Liu, Y., Cao, J., Cheng, G., 2022a. Que Zui tea ameliorates hepatic lipid accumulation and oxidative stress in high fat diet induced nonalcoholic fatty liver disease. *Food Res. Int.* 156, 111196.
- Zhang, X., Su, M., Du, J., Zhou, H., Li, X., Zhang, M., Hu, Y., Ye, Z., 2022b. Profiling of naturally occurring proanthocyanidins and other phenolic compounds in a diverse peach germplasm by LC-MS/MS. *Food Chem.* 403, 134471.
- Zhong, S., Li, J., Wei, M., Deng, Z., Liu, X., 2023. Fresh and browned Lotus root extracts promote cholesterol metabolism in FFA-induced HepG2 cells through different pathways. *Foods* 12 (9), 1781.